National School on Neutron and X-ray Scattering
August 15-29, 2004
Argonne National Laboratory

Reflectometry Applications

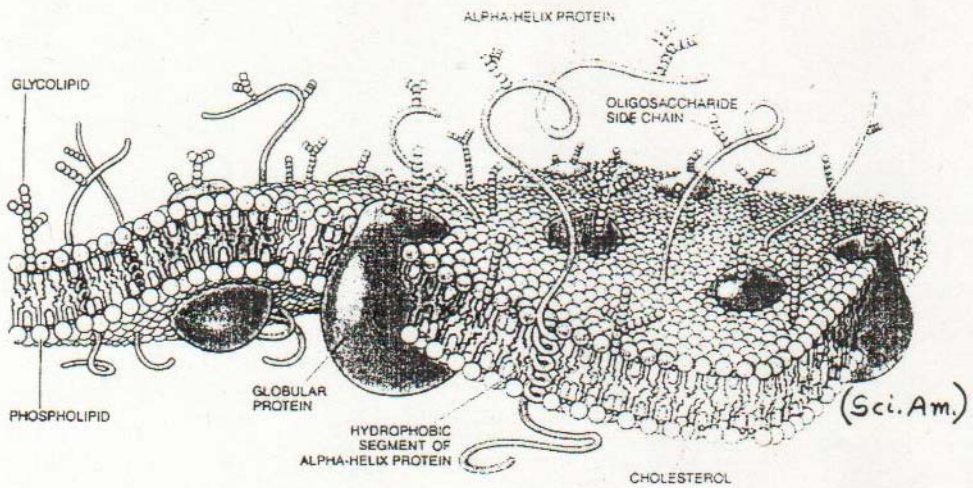

C.F.Majkrzak

National Institute of Standards and Technology

NIST CENTER FOR NEUTRON RESEARCH

Surfaces and Interfaces: NEUTRON REFLECTOMETRY

****

PRINCIPAL RESEARCH TOPICS

****

* POLYMER INTERFACES

  - POLYMER BRUSH STRUCTURE
  - WETTING OF LIQUIDS ON LIQUID SURFACES
  - ORDERING OF DIBLOCK COPOLYMER FILMS
  - POLYMER DIFFUSION IN THIN FILMS

---

* MAGNETIC SUPERLATTICES & THIN FILMS

  - INTERLAYER COUPLING
    / MAGNETIC MEDIA / (Fe/Cr)
    / SEMICONDUCTOR / (EuTe/PbTe)
    / INSULATING / (Fe & Co oxides)
    / CONDUCTING / (Co/Cu)
    / HYDROGEN CONTAINING / (Fe/V)
  - EFFECTS OF INTERFACIAL ROUGHNESS
  - DOMAIN STRUCTURE
  - GIANT MAGNETORESISTANCE (GMR) EFFECT

* LANGMUIR-BLODGETT FILMS

  - INTERDIFFUSION

  - SURFACE & INTERFACIAL ROUGHNESS

  - STRUCTURE

---

* BIOLOGICAL MEMBRANES

  - LIPID LAYER STRUCTURE

  - PROTEIN ADSORPTION

---

* ELECTROCHEMISTRY

  - INTERDIFFUSION AT ELECTRODE BOUNDARIES

  - CORROSION

---

* SUPERCONDUCTIVITY

  - MAGNETIC FIELD PENETRATION DEPTH IN THIN FILMS

  - VORTEX STRUCTURE IN THIN FILMS

---

* DIFFUSION PROCESSES

  - LIGHT ATOMS

  - ISOTOPES

* Neutron reflection/diffraction complements other nonlocal probes, e.g., electron and x-ray diffraction, as well as more local microscopic probes such as STM and AFM.

* "Real" space and reflectivity are connected through the relation

$$|r|^2 = \left| \frac{4\pi}{iQ} \int_{-\infty}^{+\infty} \Psi_F \, \rho(z) \, \Psi_I \, dz \right|^2$$

$$\rho(z) = N b$$

$$Q = \frac{4\pi \sin\theta}{\lambda}$$

(IN BORN APPROXIMATION, INTEGRAND $\longrightarrow \rho(z) e^{iQz}$

Although scattering is inherently nonlocal, detailed microstructural information can be extracted through proper mathematical analysis.

* significant differences in effective neutron scattering powe exist for various isotopes, most notably H and D, and atoms with magnetic moments:

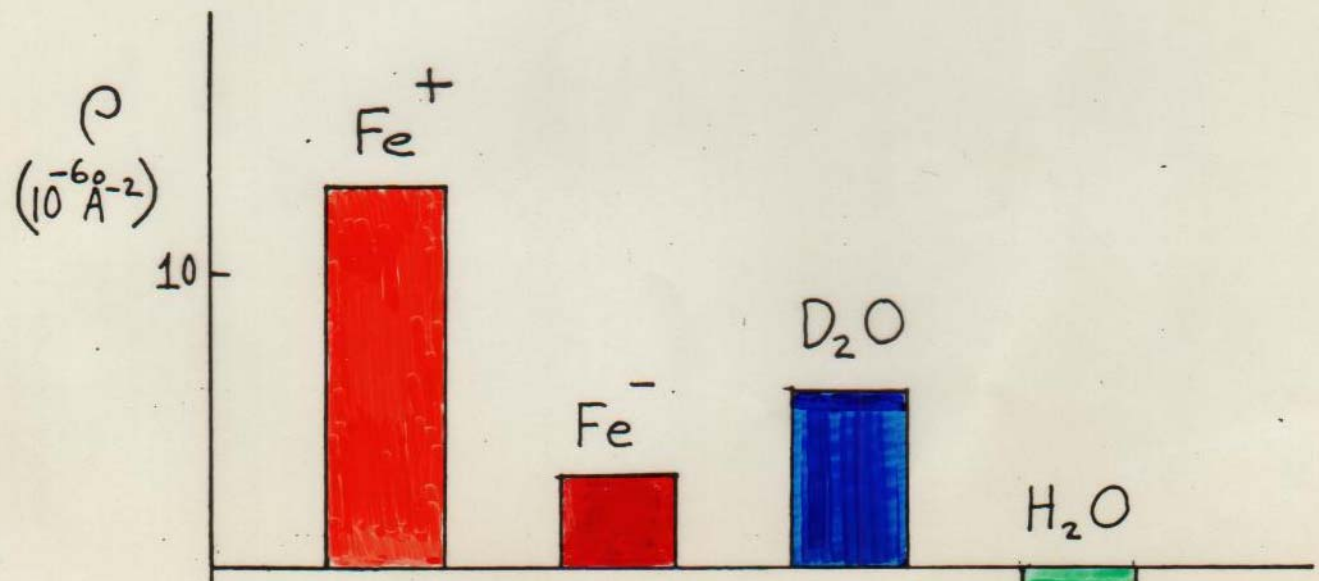

POLYSTYRENE / PMMA

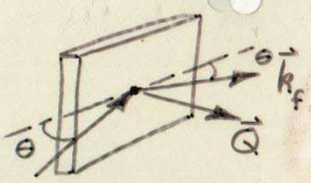

$Q = 2k \sin\theta$

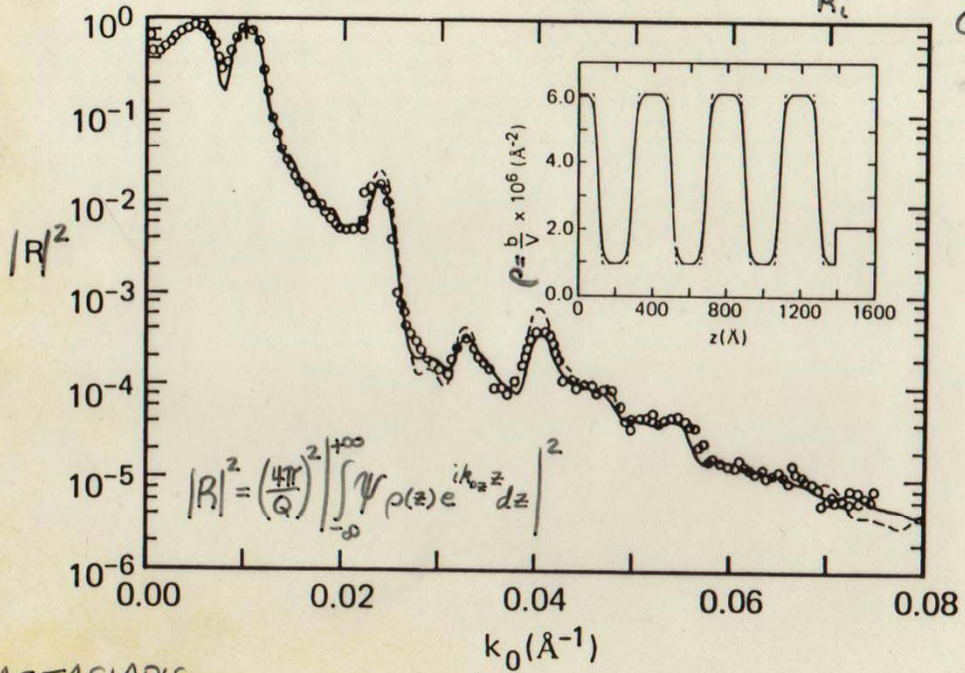

S. ANASTASIADIS
T. RUSSELL
et al.

INTERFACIAL WIDTH
54. ± 2. Å

Structure of symmetric polyolefin block copolymer thin films

Mark D. Foster,[a] Mohan Sikka, Navjot Singh, and Frank S. Bates
Department of Chemical Engineering and Materials Science, University of Minnesota, Minneapolis, Minnesota 55455

Sushil K. Satija and Charles F. Majkrzak
National Institute of Standards and Technology, Reactor Radiation Division, Gaithersburg, Maryland 20899

(Received 5 February 1992; accepted 27 February 1992)

The microstructure of thin films of nearly symmetric poly(ethylene–propylene)–poly(ethylethylene) (PEP-PEE) diblock copolymers ($f = 0.55$, where f is the volume fraction of PEP) was characterized by neutron reflectometry (NR). A symmetric film structure in which the PEE block segregates preferentially to both interfaces is observed above and below the bulk order–disorder transition (ODT). Measurements at room temperature for several chain lengths, N, provide a real-space picture of the change in interdomain interfacial profiles associated with the crossover between the strong and weak segregation limits. The polymer/air and substrate/polymer interfaces are observed to induce an ordered microstructure even when the center of the film is disordered. The characteristic dimension of this near surface microstructure is larger than the corresponding bulk value for values of χN lying between those of the bulk Gaussian-to-stretched-coil and order–disorder transitions, where χ is the segment–segment interaction parameter. This behavior is attributed to the correlation of large amplitude composition fluctuations in the film with the interfaces. A mean-field behavior prevails for $\chi N < (\chi N)_{\mathrm{GST,bulk}}$, where some preferential segregation occurs at the interfaces, but the characteristic dimension once again matches that in the bulk.

I. INTRODUCTION

In recent years interest has grown rapidly in understanding how the presence of symmetry breaking interfaces affects the microstructure and transitions of systems that can undergo order–order and order–disorder transitions. Two types of systems where considerable study has already

ly linked at one point. The overall degree of polymerization, N, the fraction of block A in the chain, f, the A–B segment–segment (Flory–Huggins) interaction parameter χ, are generally assumed to dictate the phase behavior of bulk block copolymers. At equilibrium the melt microstructure is that which minimizes the overall free energy and the transition

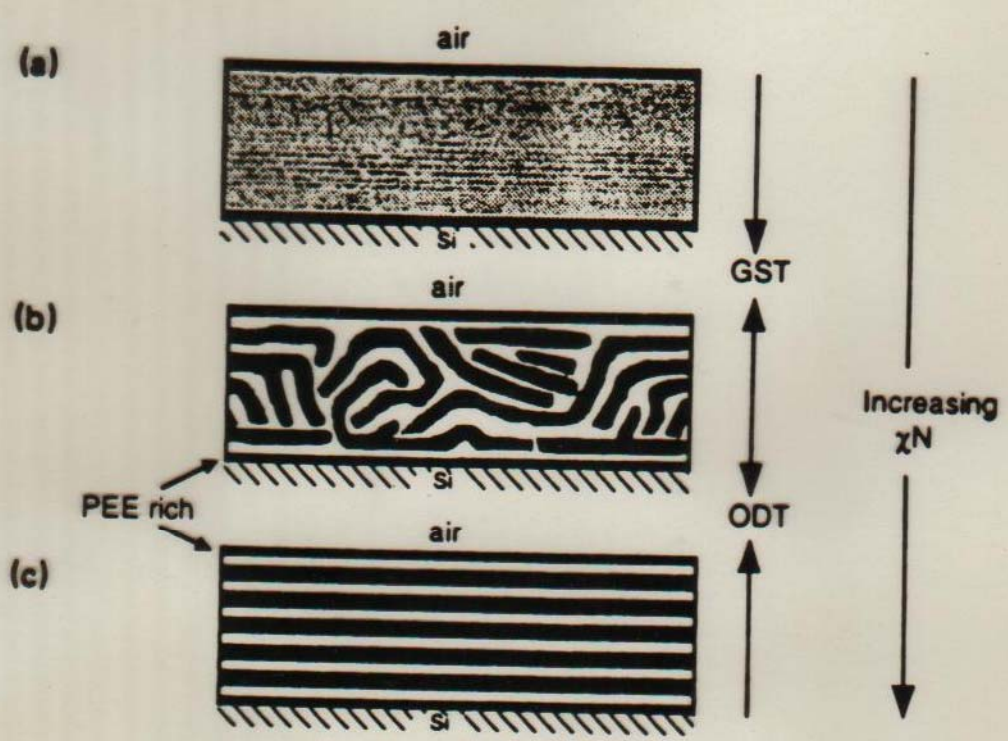

G. 5. Thin film morphologies for symmetric PEP–PEE diblock copo-
ners. (a) Interfacial segregation of PEE occurs for $\chi N < (\chi N)_{GST}$.
e center of the film is spatially homogeneous. (b) For
$N)_{GST} < (\chi N) < (\chi N)_{ODT}$ the film contains a microstructured morphol-
y that is oriented at the film interfaces. The range of the orientational
rrelation increases with increasing (χN). (c) A lamellar microstructure
t is highly oriented with the film interfaces exists when
$N) > (\chi N)_{ODT}$.

In a second series of measurements, the disordering of the room temperature (23 ± 2 °C) microstructure with decreasing chain length is observed. Reflectivity curves for six chain lengths are shown in Fig. 8. While some of the important trends in structural change with N are readily apparent from the raw data, the reader should recall that two different

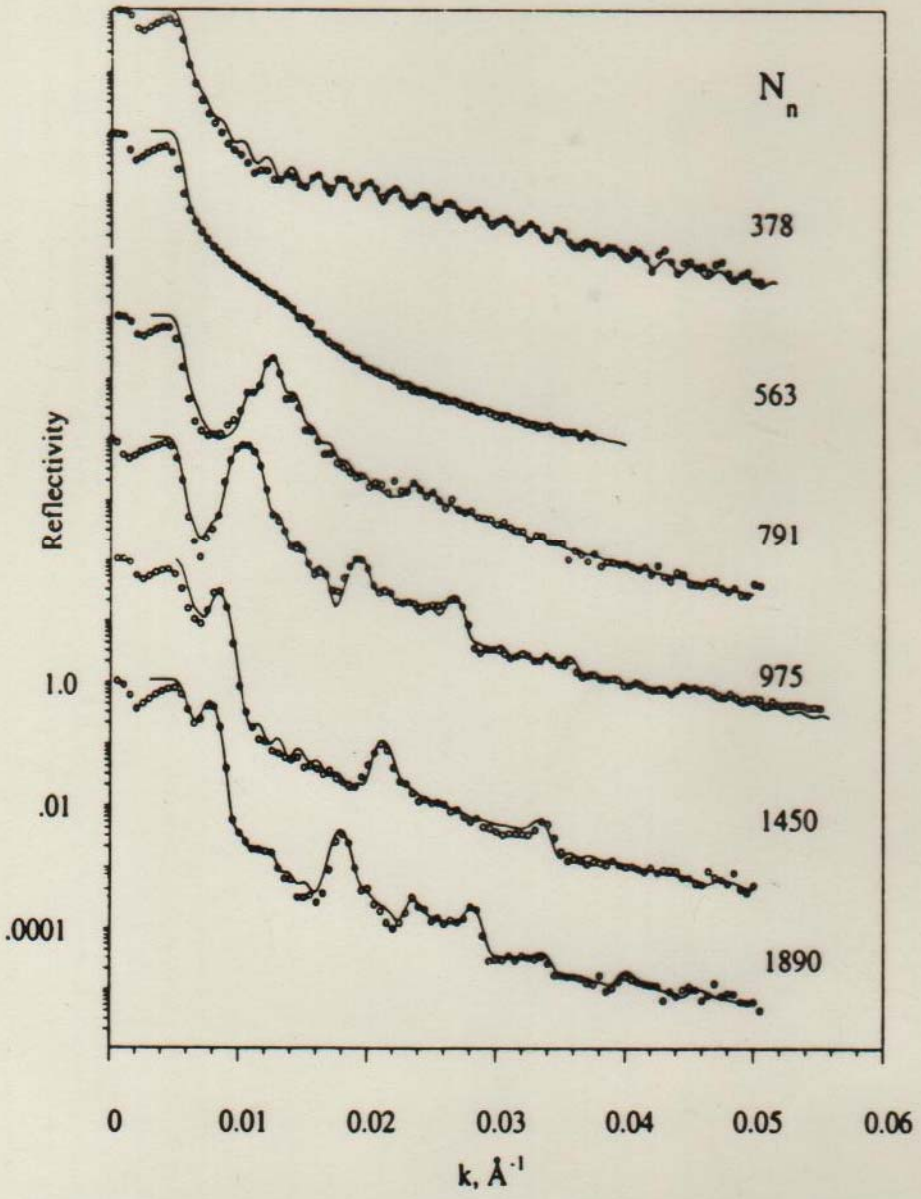

FIG. 8. Reflectivity data for six PEP–PEE chain lengths and the corresponding model curves used to infer concentration profiles illustrated in Fig. 9. The results for $N < 1890$ have been shifted vertically. Poor agreement between the model curves and data in the vicinity of the critical wave vector stems from an experimental artifact that also produces the apparent lack of total reflectivity for $k \lesssim k_c$ (Ref. 32).

present in the $N = 975$ s
after correction for the p
a domain size of 566 ±

As the chain length
out to higher values of
size. The peaks also bec
since the contrast in thi
$N = 1890$ sample, this s
what less sharply define
chain length are accom
flectivity curve. Once N
order Bragg peak is bare
become quite broad. Thi
film. For $N = 563$ the re
defined first order peak
change in the Bragg pea
tive change in order. Up
lecular weight the remai
pushed out to considera
enhanced somewhat sim
a higher contrast. The ap
the curve is due only t
these are "Kiessig" fring
the films's order.

These extensive qua
performing detailed ana
shown graphically in Fi
centration profiles corre
ties plotted as solid curv
prove these profiles to b
consistency reassure us
was collected with two
several real space profil
trend in structure. This
markable in that it depi
the strongly segregated
ture. Such a picture is n
surements. At the highe
volume fractions in the
tially 1.0 and 0.0, respe
relatively sharp. This sit

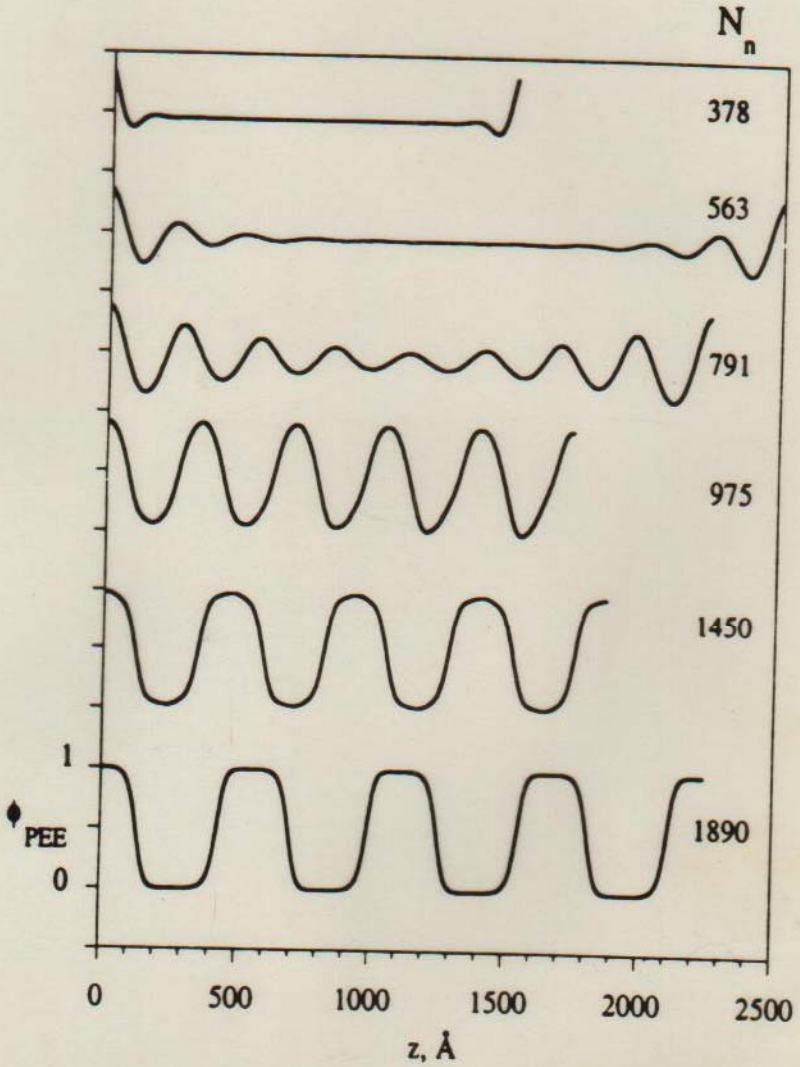

FIG. 9. Real space concentration profiles corresponding to the model curves shown in Fig. 8.

Fig. 5(c). The interface width may be characterized by the inverse of the slope of a tangent to the profile at the interface midpoint, as suggested by Helfand,[9]

$$a_I \equiv \left(\frac{dz}{d\phi}\right)_{\phi=0.5}. \tag{2}$$

STRUCTURAL STUDIES OF LANGMUIR-BLODGETT FILMS

DAVE WIESLER (NIST)
LEV FEIGIN (MOSCOW)
WOLFGANG KNOLL (PLANCK)
ALBERT SCHMIDT (PLANCK)
MARK FOSTER ET AL. (AKRON)

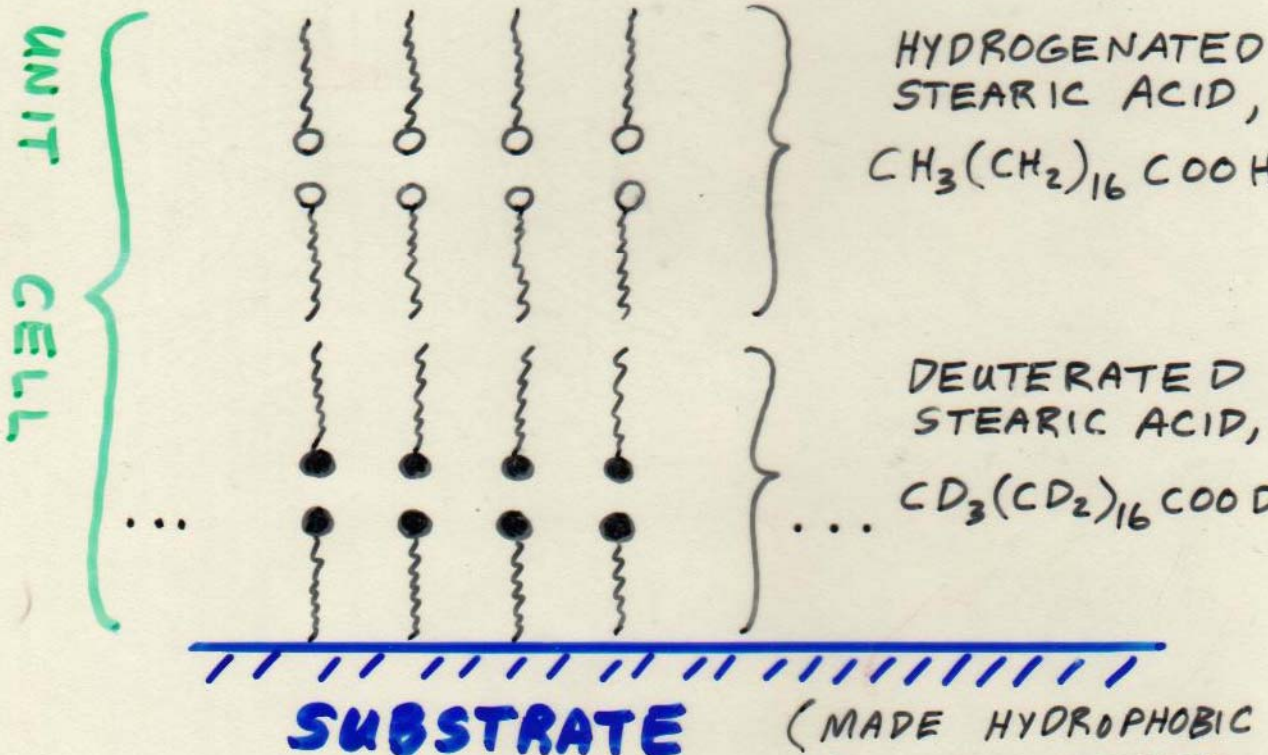

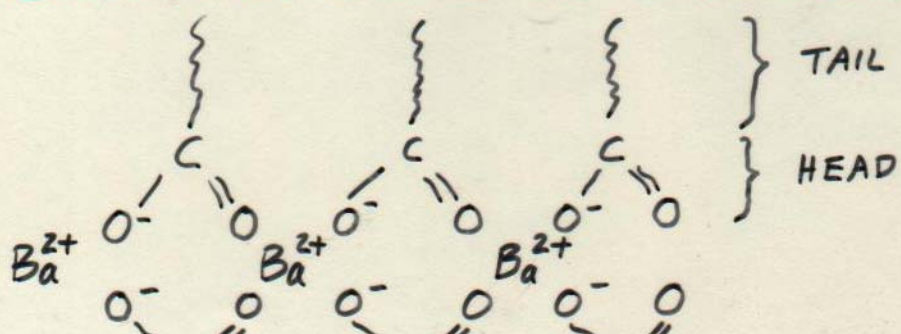

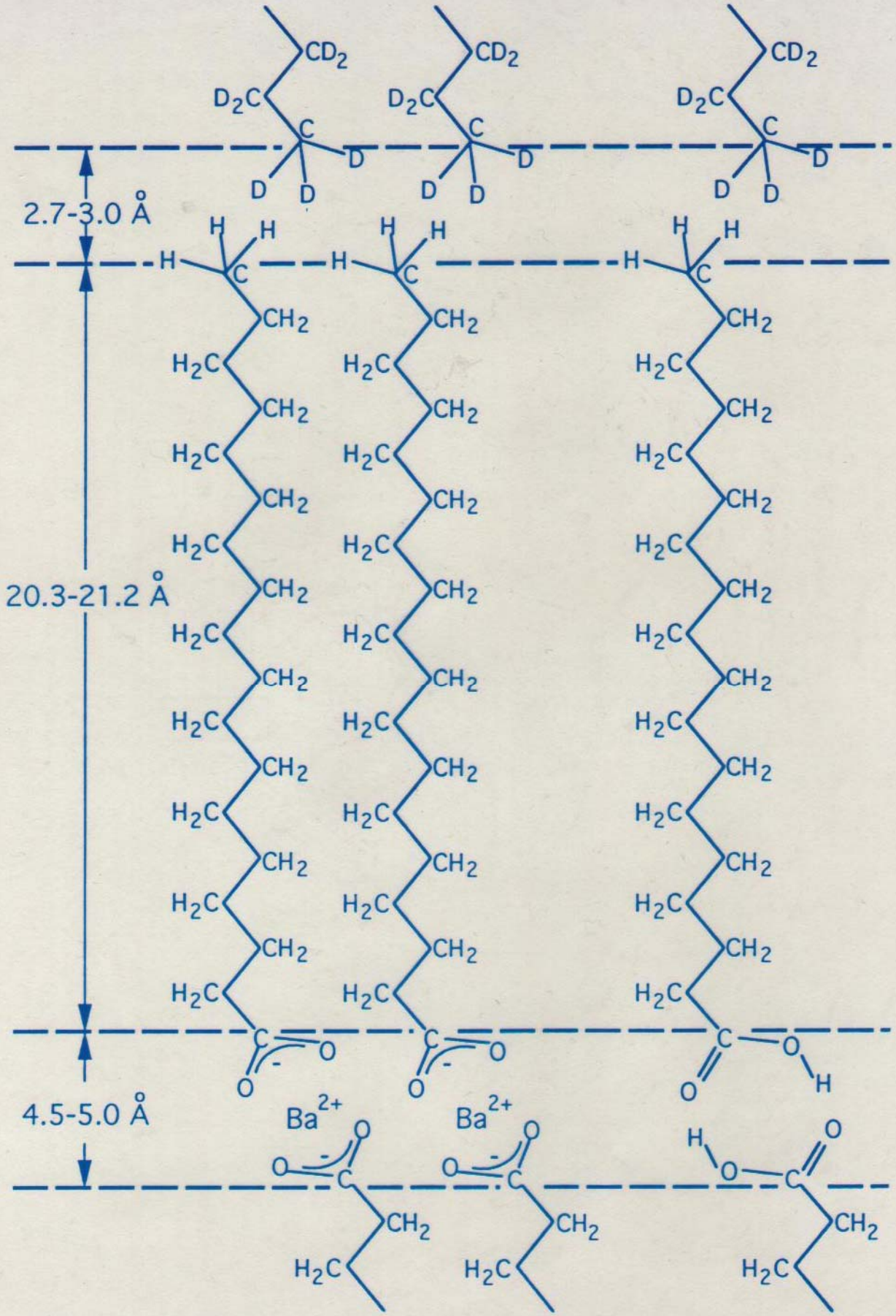
2.7-3.0 Å
20.3-21.2 Å
4.5-5.0 Å
Ba2+
Ba2+

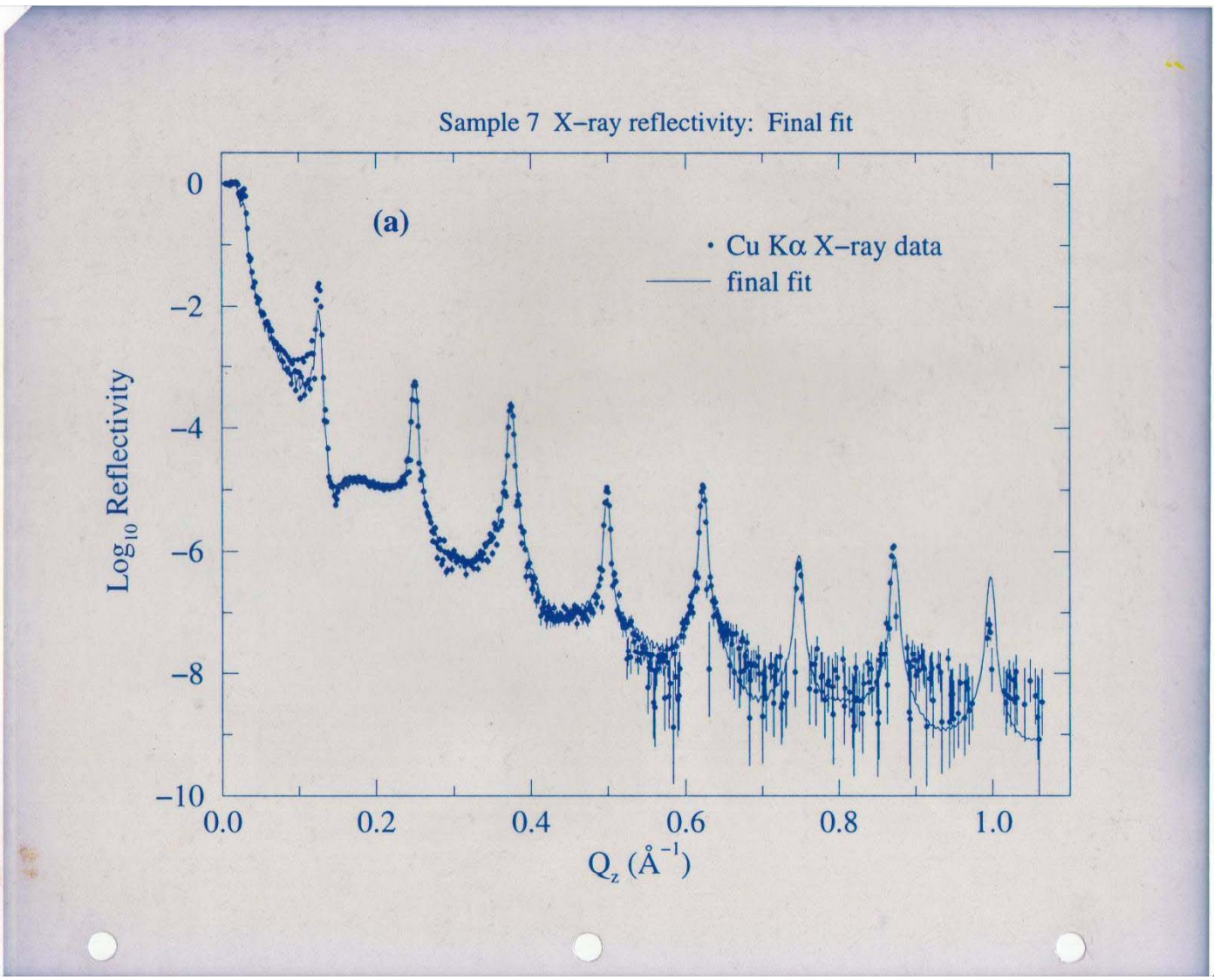
Sample 7 X–ray reflectivity: Final fit
(a)
• Cu Kα X–ray data
final fit
Log10 Reflectivity
0
−2
−4
−6
−8
−10
0.0
0.2
0.4
0.6
0.8
1.0
Qz (Å−1)

LANGMUIR-BLODGETT FILM
(20 BILAYERS OF Ba STEARATE)

D. WIESLER, L. FEIGIN, C.F. MAJKRZAK, J. ANKNER, T. BERZINA, & V. TROITSKY

Sample 7 Neutron reflectivity: Final fit

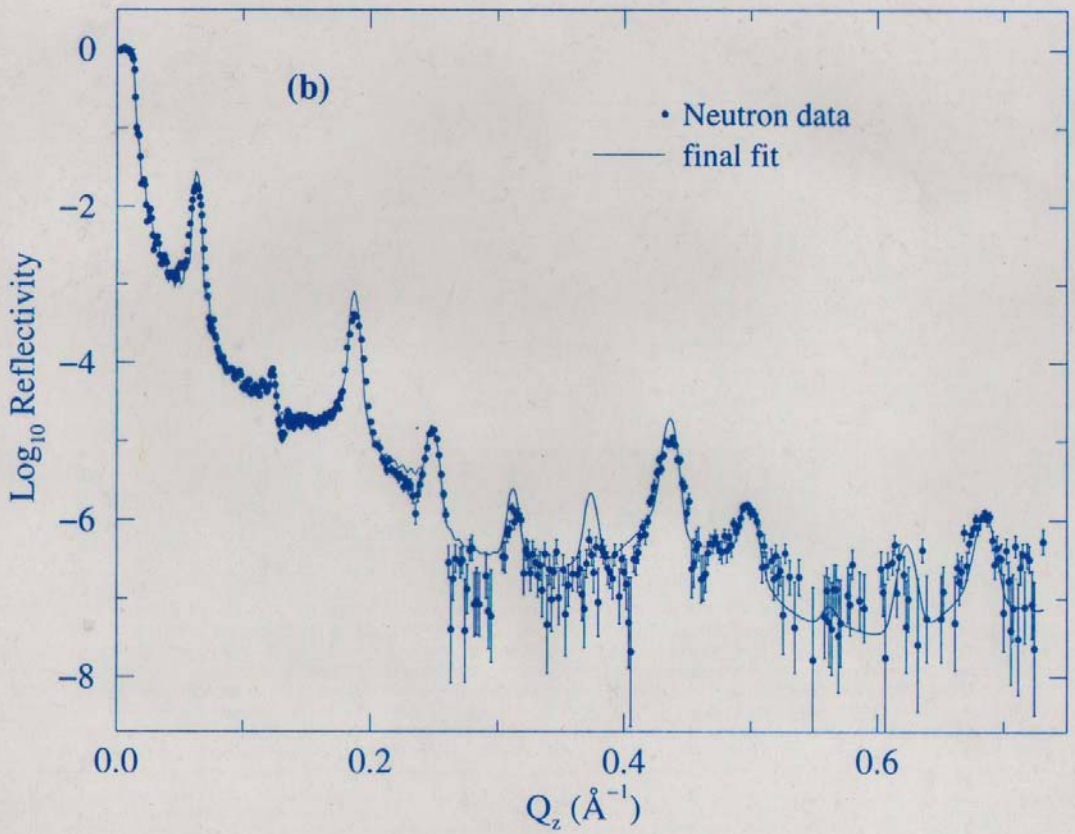

Ba STEARATE LB FILM

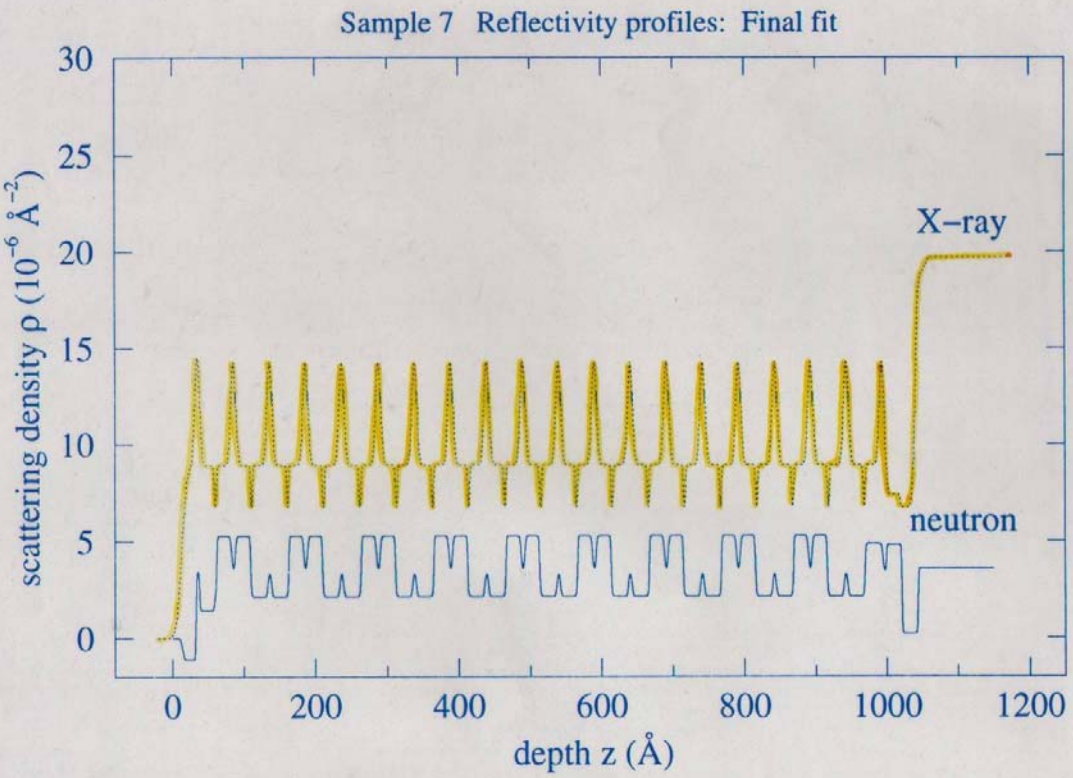

Neutron Reflectivity Studies of Surfactants at Electrode Surfaces

Knowledge of the forces that control the assembly of surfactant molecules at the solid-liquid interface is vital for traditional fields such as detergency, flotation, oil recovery and tribology [1]. Thin organic films deposited at solid surfaces also find application in the fabrication of optoelectronic devices, sensors, biosensors, and chemically modified electrodes [2]. It has long been established that the assembly of surfactants at the solid-liquid interface depends on the charge at the solid surface [3, 4]. For example, the spreading of vesicles into a phospholipid bilayer requires that the surface of the solid be negatively charged and hydrophilic.

However, the present understanding of the role played by charge on the interaction of a surfactant molecule with the electrified solid surface is far from being complete. Electrochemistry provides a unique opportunity to study the effect of the charge on the properties of amphiphilic and ionic surfactants at the charged solid-liquid interface [5]. When an organic film is deposited on a gold electrode, the charge density at the metal surface may be varied from about 30 $\mu C/cm^2$ to about 40 $\mu C/cm^2$. This magnitude of charge generates electric fields on the order of 10^{10} V/m. Such a field interacts with polar molecules in the membrane. By changing the sign of the charge one can use attractive or repulsive forces. In this manner, by turning a knob on a control instrument one can force phase transitions in the film of organic molecules or force surfactants to desorb or re-adsorb on the surface.

We have recently employed electrochemical techniques, atomic force microscopy, and neutron reflectivity to study the field driven transformations of thin films formed by a model anionic surfactant, sodium dodecyl sulfate (SDS), at the surface of a gold electrode [6]. Figure 1 shows how the surface concentration of SDS at the Au electrode surface changes with the electrode potential. A convenient way to interpret these data is to look at the electrode potential as an operational variable that can be easily adjusted using a control instrument.

Figure 1 shows that the character of SDS adsorption is strongly influenced by the charge on the metal. At sufficiently negative potentials SDS molecules are totally desorbed from the electrode surface. At moderate negative

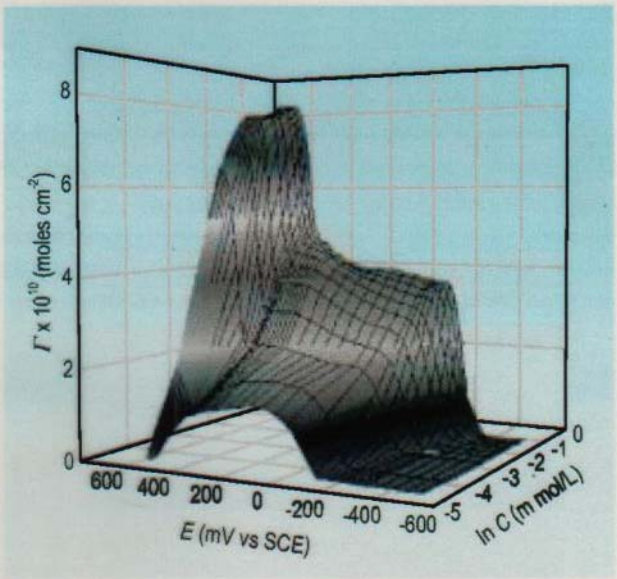

FIGURE 1. Three dimensional plots of the surface concentration of SDS as a function of electrode potential measured versus the calomel reference electrode (SCE) and the logarithm of the bulk SDS concentration.

charge densities SDS forms a film characterized by a limiting surface concentration 4.0×10^{-10} mol cm^{-2}. When the metal surface is positively charged the surface concentration of SDS increases to 8.1×10^{-10} mol cm^{-2}.

Neutron reflectivity experiments carried out on the NG-7 reflectometer were employed to determine the structure of the film formed by SDS at different charge densities at the gold surface. Thin layers of chromium (≈ 20 Å) and gold (≈ 80 Å) were sputtered onto the crystal quartz substrate. After cleaning, the crystal was mounted on a specially constructed Teflon® cell [7]. The cell had ports for the counter (gold foil) and reference electrodes (Ag/AgCl, $E \approx -40$ mV versus SCE). D_2O (99.9 % molecular fraction) was used as a solvent in reflectivity studies.

Figure 2a shows the neutron reflectivity data determined for SDS adsorption at various electrode potentials, and Fig. 2b shows the scattering length density profiles calculated from the reflectivity curves. The neutron reflectivity data are consistent with electrochemical measurements. They show that at very negative potentials the gold solution interface is free from hydrogenated species. When

I. Burgess, V. Zamlynny, G. Szymanski, and J. Lipkowski
Department of Chemistry and Biochemistry
University of Guelph
Guelph, ONT N1G 2W1, Canada

J. Majewski and G. Smith
Los Alamos National Laboratory
Los Alamos, NM 87545

S. Satija and R. Ivkov
NIST Center for Neutron Research
National Institute of Standards and Technology
Gaithersburg, MD 20899-8562

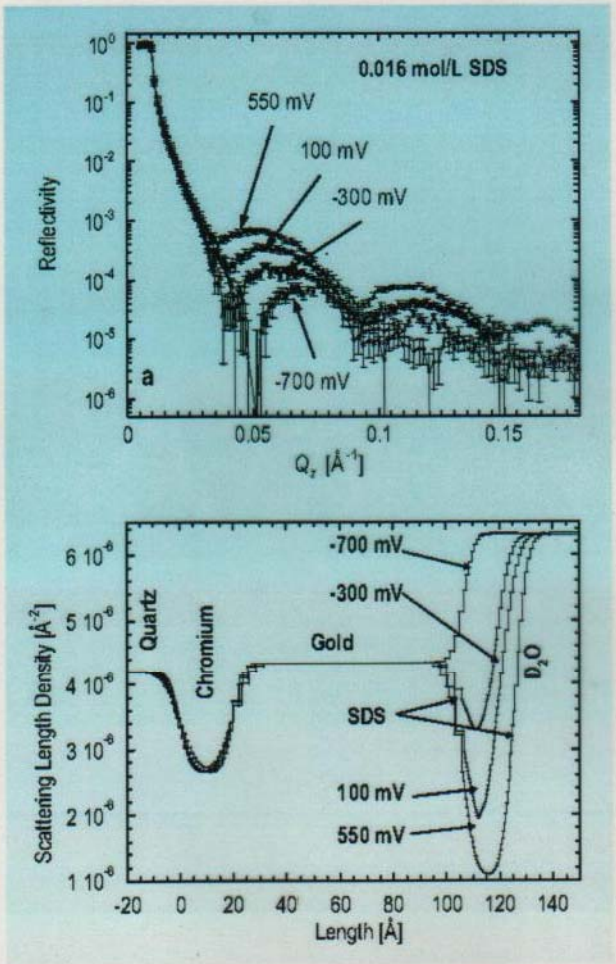

FIGURE 2. (a) Normalized neutron reflectivity curves for a Au/Cr-coated quartz substrate in 0.016 mol/L SDS in D_2O. (b) Scattering length density profiles of the interface as determined from the fitting procedure.

the potential increases, the film of hydrogenated species appears at the electrode surface. The thickness of this film increases, and the scattering length density progressively decreases, with increasing potential. When combined with the results of electrochemical measurements and atomic force imaging, the neutron reflectivity data allow the determination of the structure of the film formed at different charge densities. At small or moderate negative charge densities SDS molecules form a hemimicellar film that consists of hemicylindrical stripes, as first observed by Manne [4]. The packing of SDS molecules in a cross section of that hemicylinder is shown schematically in Fig. 3 (top). At positive charge densities the hemimicellar state is transformed into the interdigitated bilayer schematically shown in Fig. 3 (bottom).

The results of this study demonstrate the need for the use of neutron reflectometry to study adsorption and phase transitions in films of surfactants adsorbed at the solid-solution interface. Specifically, they show that when neutron reflectivity measurements are combined with electrochemical studies and atomic force microscopy, they provide unique opportunities to study different stages involved in the interaction of surfactants with solid surfaces.

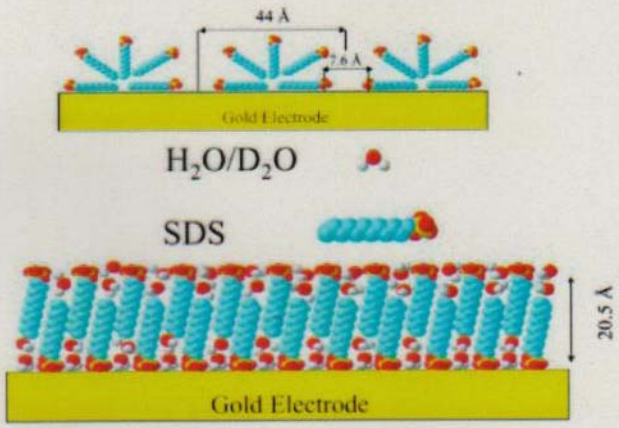

FIGURE 3. Models of SDS adsorption at the Au-solution interface: (top) cross section of hemicylindrical aggregates observed at moderately negative charge densities; (bottom) interdigitated bilayer observed at positive charge densities.

References

[1] A.W. Adamson, Physical Chemistry of Surfaces, 5th ed., John Wiley & Sons, New York (1990).

[2 E. Sackmann, Science **271**, 43 (1996).

[3] P. Chandar, P. Somasundaran, N. J. Turro, J. Colloid Interface Sci. **117**, 31 (1987).

[4] S. Manne, Progr. Colloid Polym. Sci. **103**, 226 (1997).

[5] D. Bizzotto, J. Lipkowski, J. Electroanal. Chem. **409**, 33 (1996).

[6] V. Zamlynny, I. Burgess, G. Szymanski, J. Lipkowski, J. Majewski, G. Smith, S. Satija, and R. Ivkov, Langmuir **16**, 9861(2000).

[7] I. Burgess, V. Zamlynny, G. Szymanski, J. Lipkowski, J. Majewski, G. Smith, S. Satija, and R. Ivkov, Langmuir **17**, 3355 (2001).

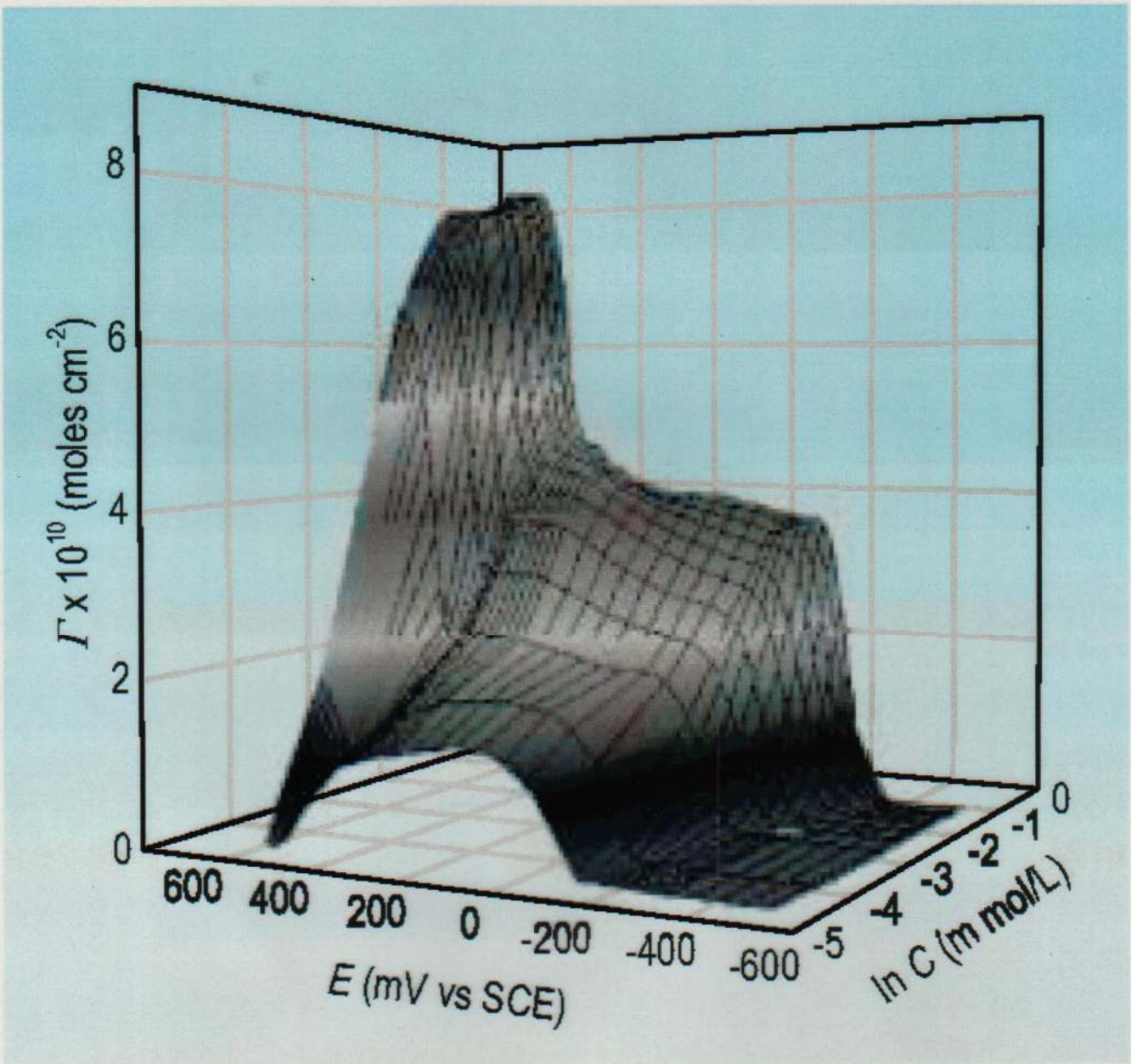

FIGURE 1. Three dimensional plots of the surface concentration of SDS as a function of electrode potential measured versus the calomel reference electrode (SCE) and the logarithm of the bulk SDS concentration.

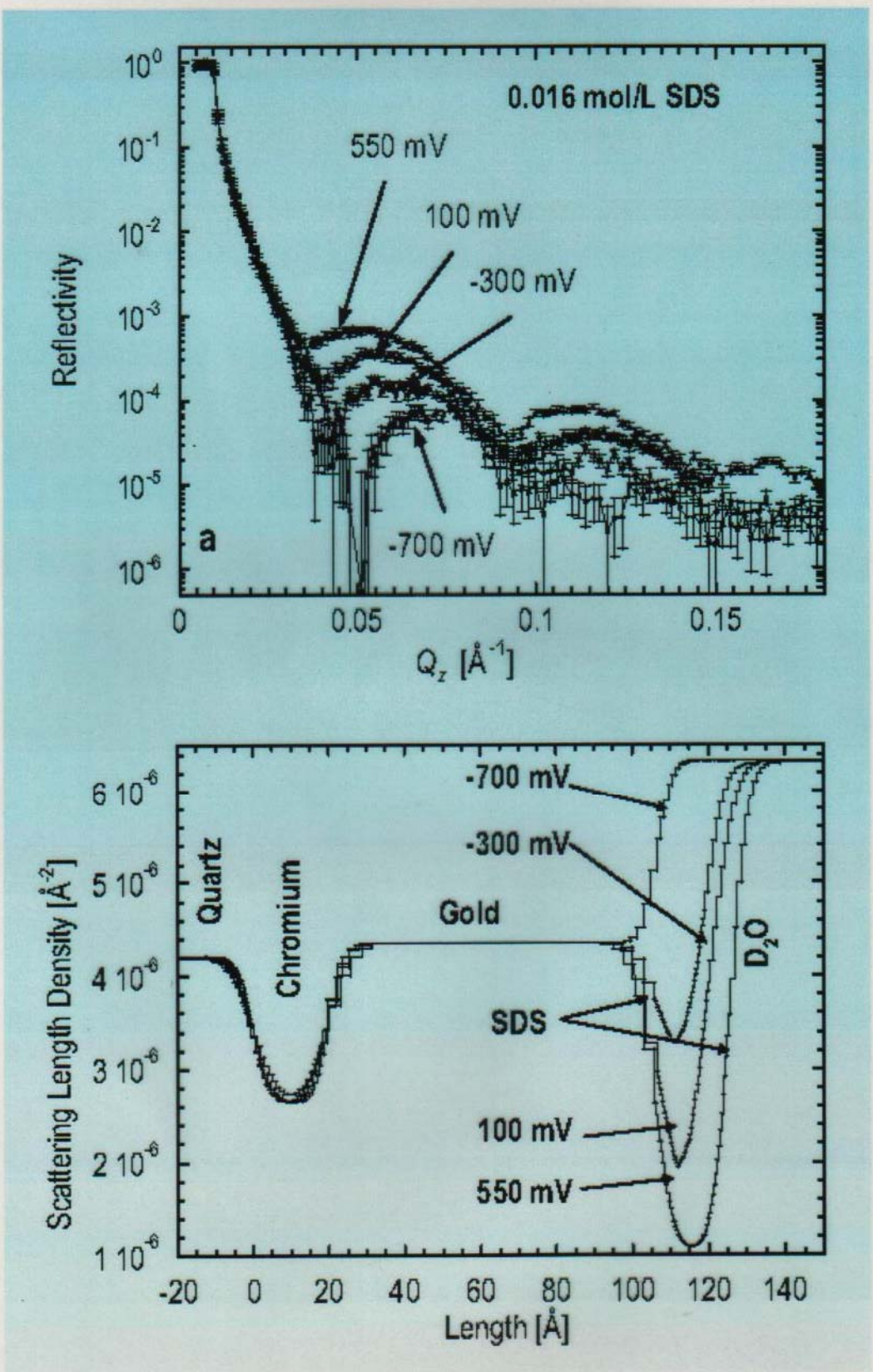

FIGURE 2. (a) Normalized neutron reflectivity curves for a Au/Cr-coated quartz substrate in 0.016 mol/L SDS in D_2O. (b) Scattering length density profiles of the interface as determined from the fitting procedure.

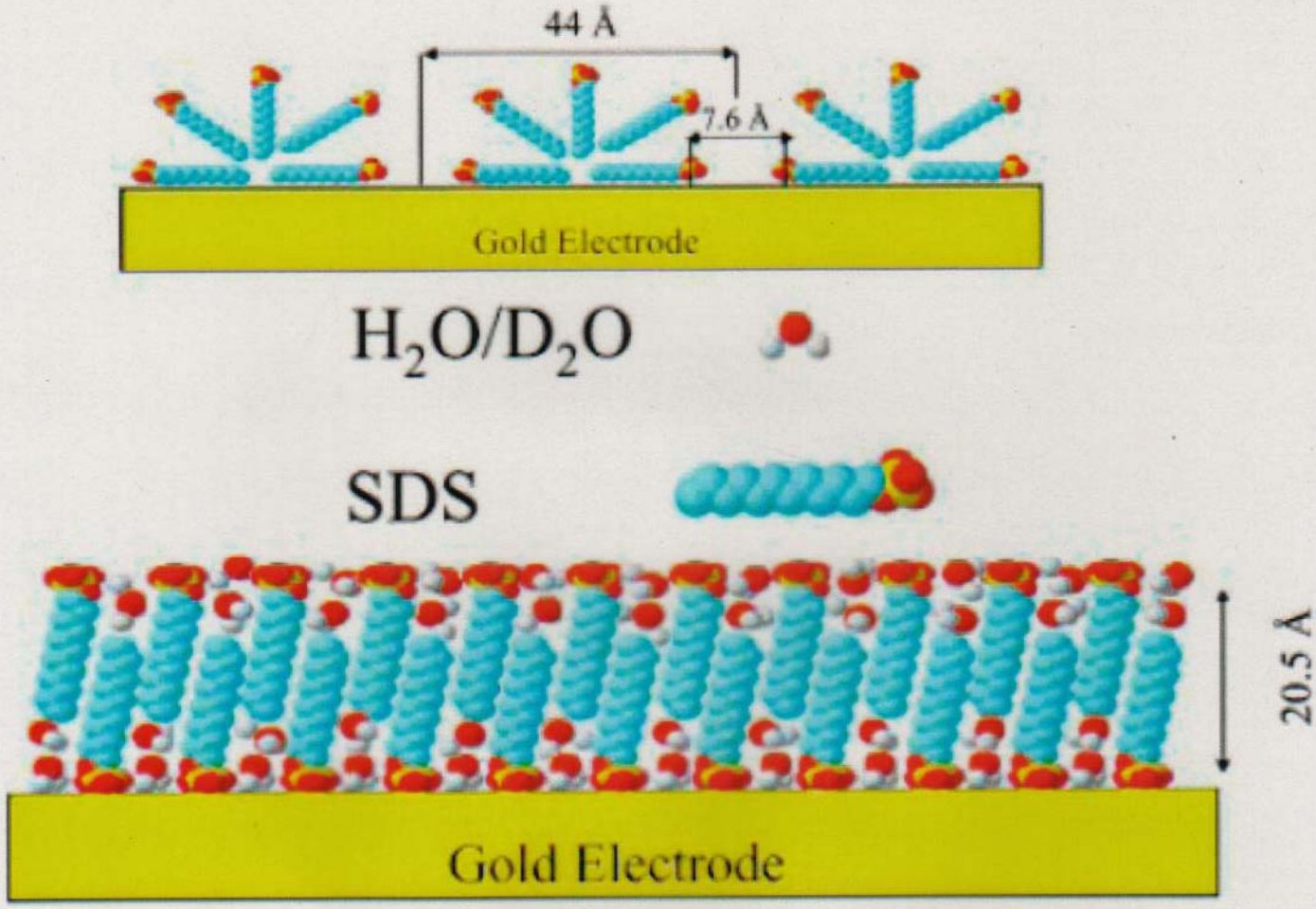

FIGURE 3. Models of SDS adsorption at the Au-solution interface: (top) cross section of hemicylindrical aggregates observed at moderately negative charge densities; (bottom) interdigitated bilayer observed at positive charge densities.

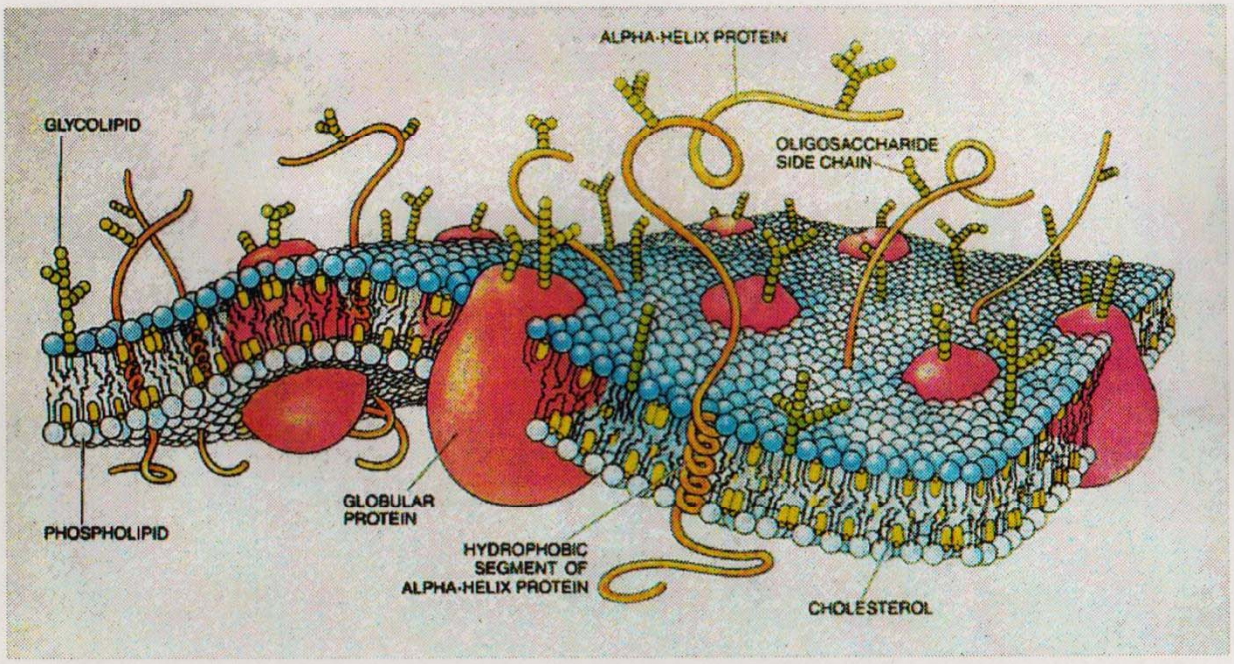

BORROWED FROM SCIENTIFIC AMERICAN

Lipid Phase Transitions

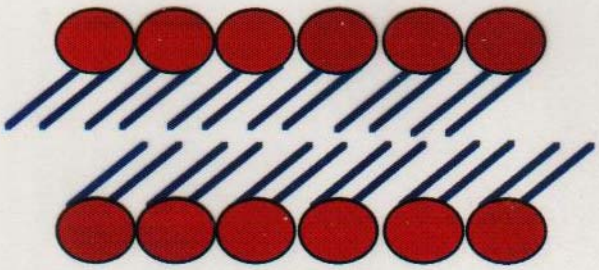

L_{β}' Crystalline
"Gel" State

Increasing Temperature

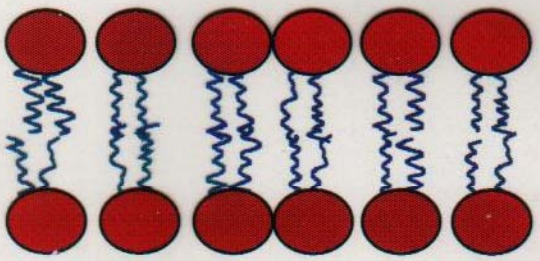

L_{α} Liquid Crystalline
Fluid State (thinner)

Transition State P_{α}
Surface Effect ?

DMPC	24 (14) °C
DPPC	42 (35) °C
DSPC	54 (49) °C

(S. KRUEGER ET AL.)

Effect of Temperature on the Neutron Reflectivity of DPPC in Si-Matched H_2O/D_2O

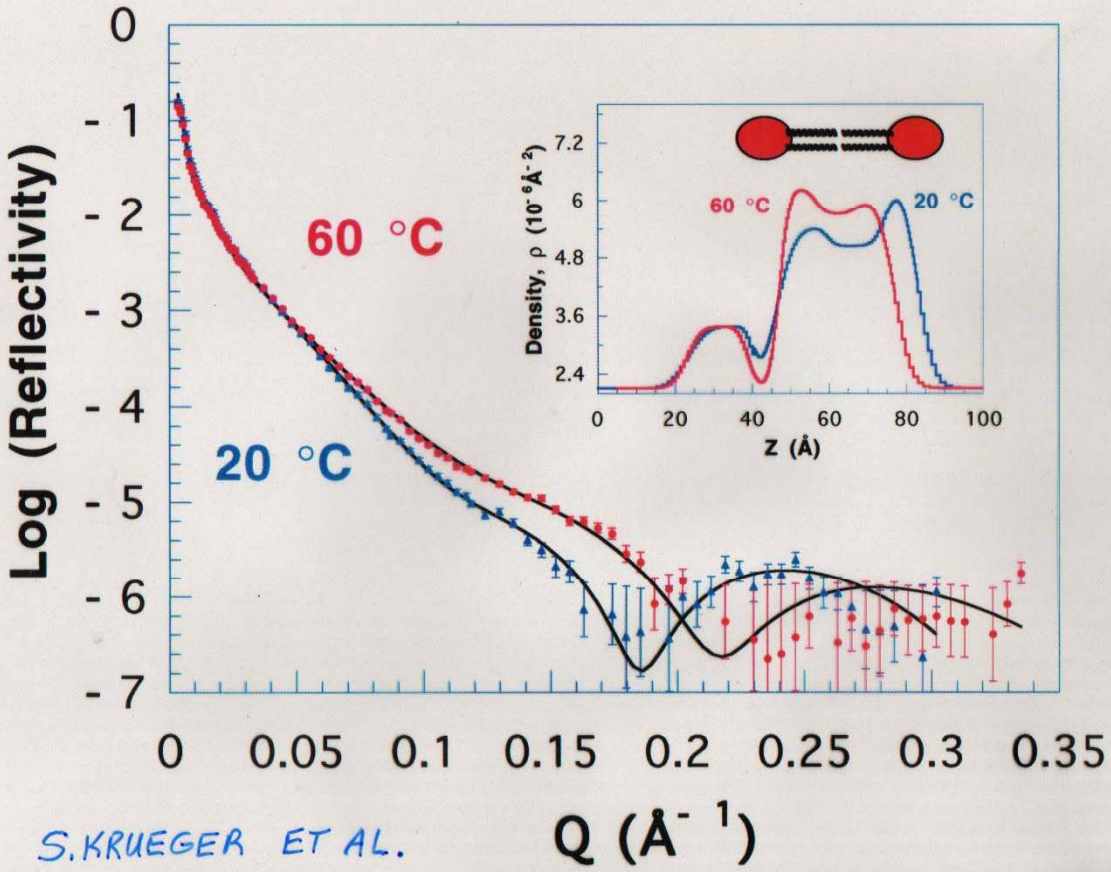

S. KRUEGER ET AL.

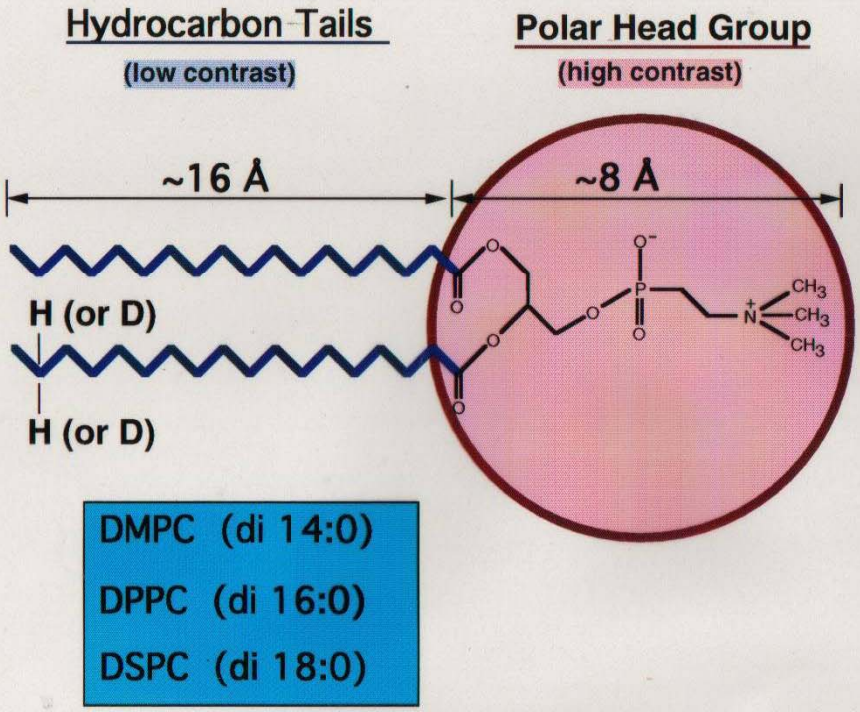

DMPC (di 14:0)

DPPC (di 16:0)

DSPC (di 18:0)

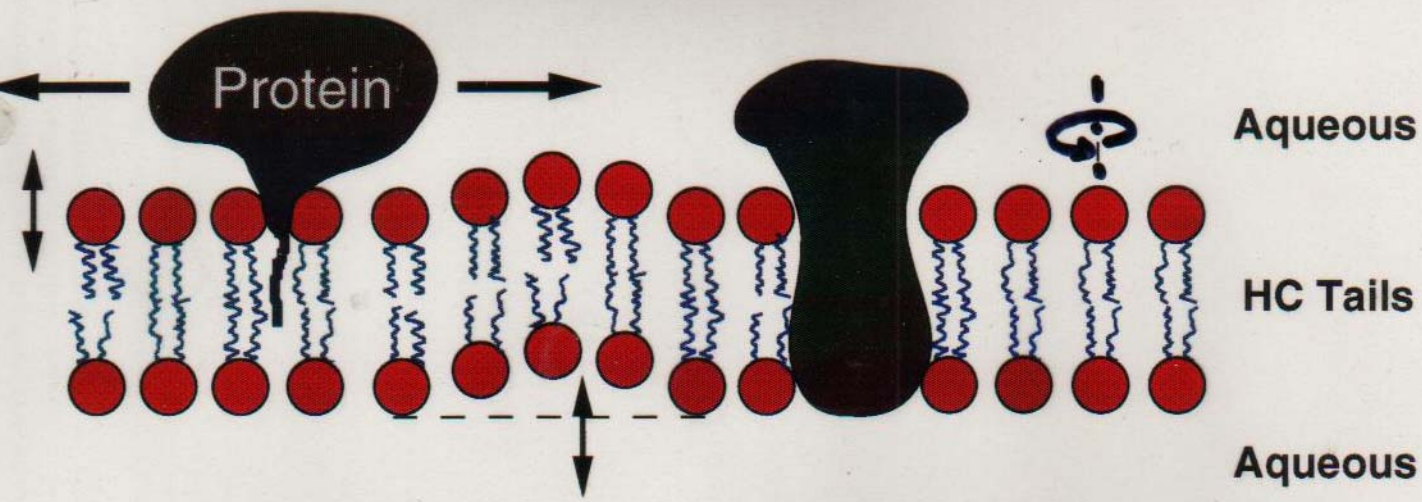

Supported Lipid Bilayers

A model system to mimic the structure and dynamics of cell membranes.

Proteins in Lipid Bilayers

- Difficult to characterize by traditional x-ray crystallography.
- Play a crucial role in cell function
  - regulate ion and nutrient transport
  - engage in binding, signalling and cell recognition
  - participate in cell fusion events.

Biosensors (Anne Plant & coworkers)

Melittin in Hybrid Bilayer Membranes

S. Krueger, A. Plant, et al., NIST (Langmuir)

- pore-forming toxin
- used as model membrane peptide
- active in HBMs

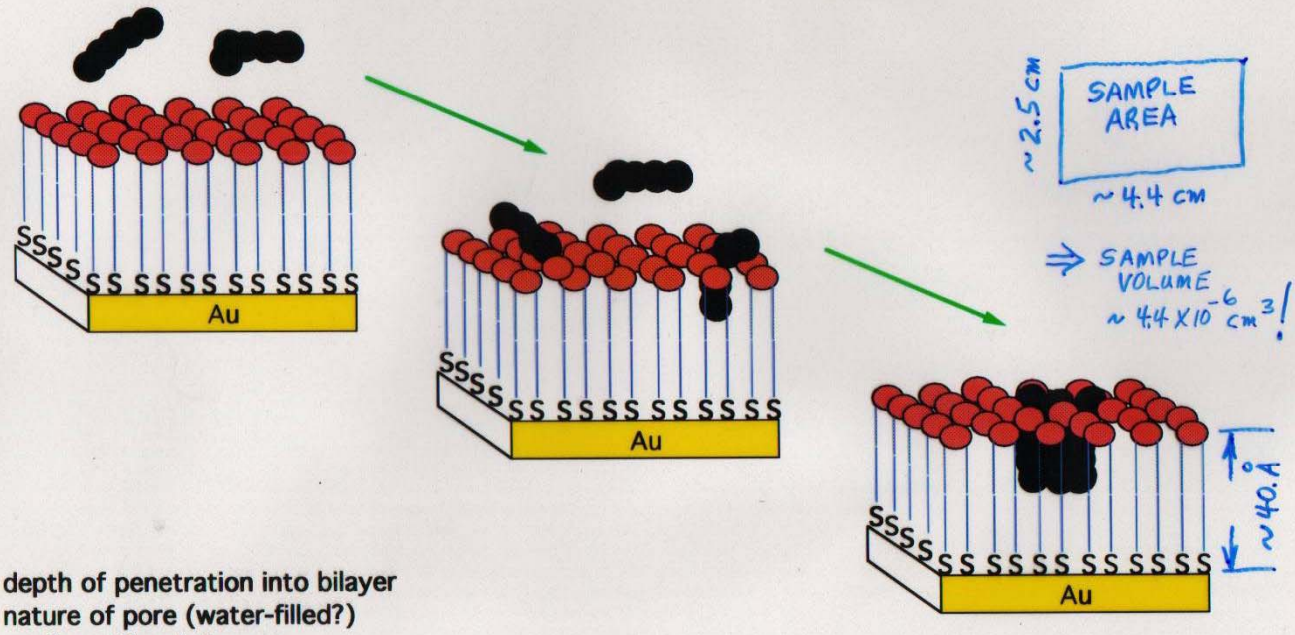

- depth of penetration into bilayer
- nature of pore (water-filled?)
- conformational changes
- random or ordered distribution?
- influence on surrounding lipids (location,conformation)

Melittin in THEO-Hybrid Bilayer Membranes

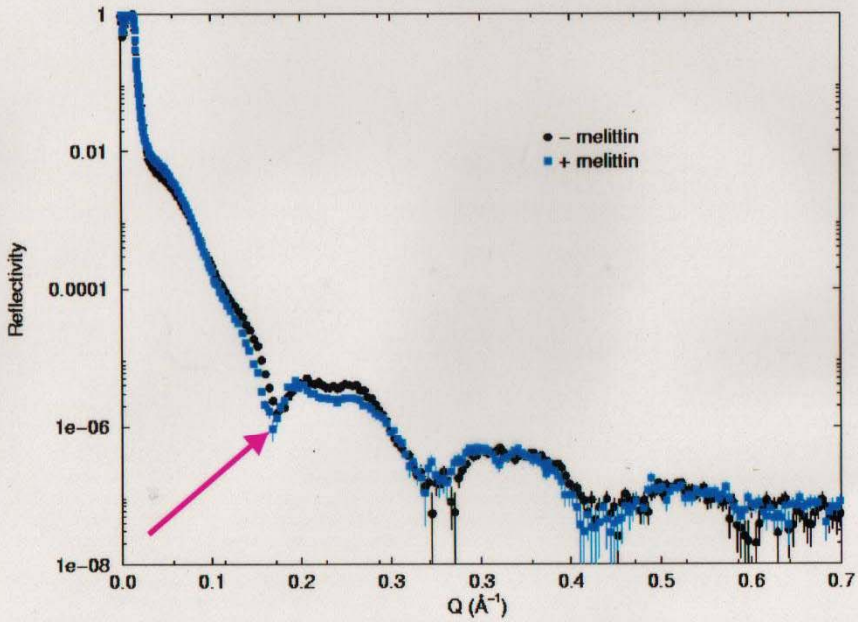

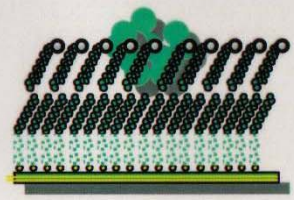

S. KRUEGER, C.F. MAJKRZAK, N.F. BERK, M. TAREK, D. TOBIAS,
V. SILIN, J.A. DURA, C.W. MEUSE, J. WOODWARD, A.L. PLANT
(Langmuir)

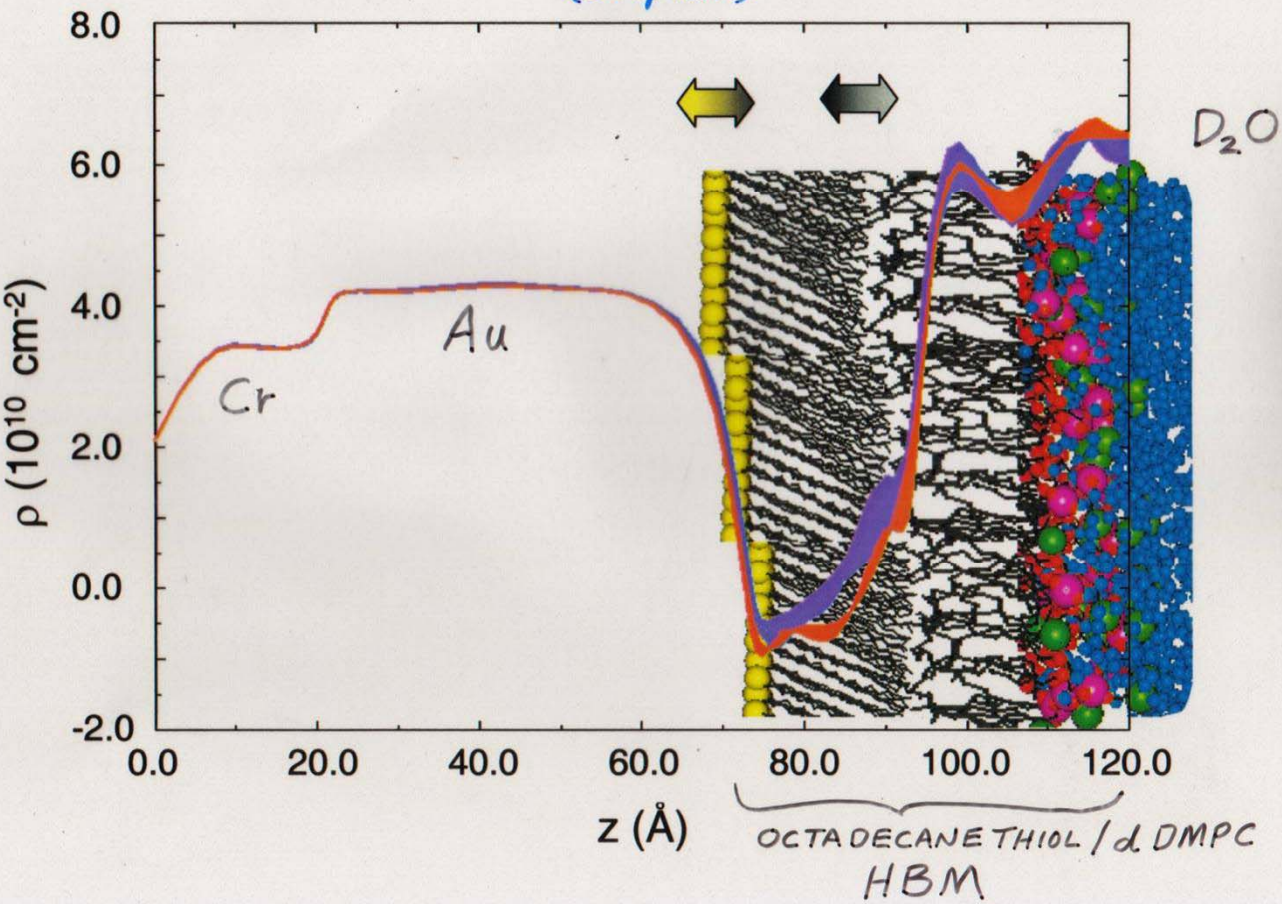

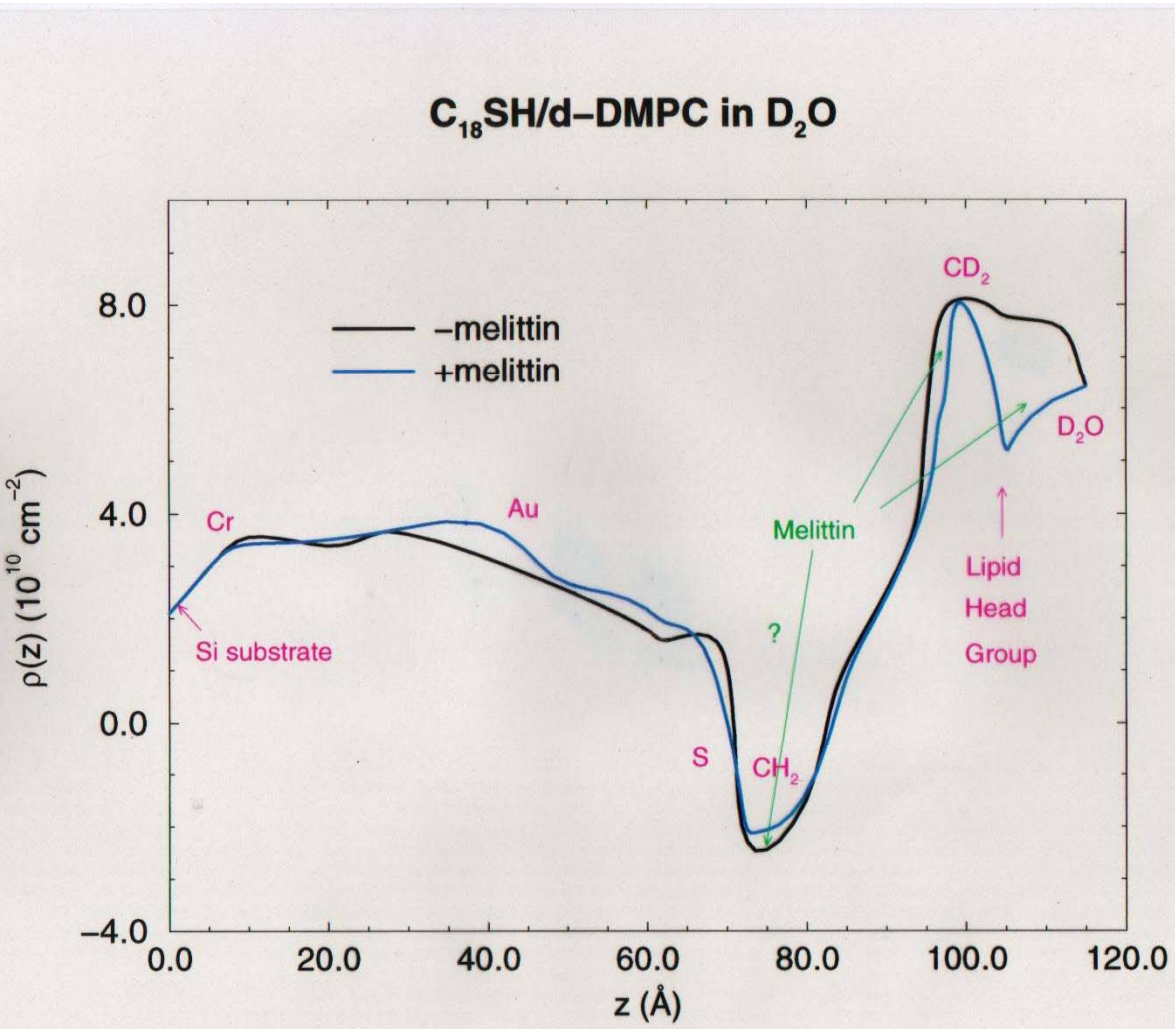
C18SH/d–DMPC in D2O
–melittin
+melittin
CD2
D2O
Cr
Au
Melittin
?
Lipid
Head
Group
Si substrate
S
CH2
8.0
4.0
0.0
–4.0
0.0
20.0
40.0
60.0
80.0
100.0
120.0
z (Å)
ρ(z) (10^10 cm^-2)

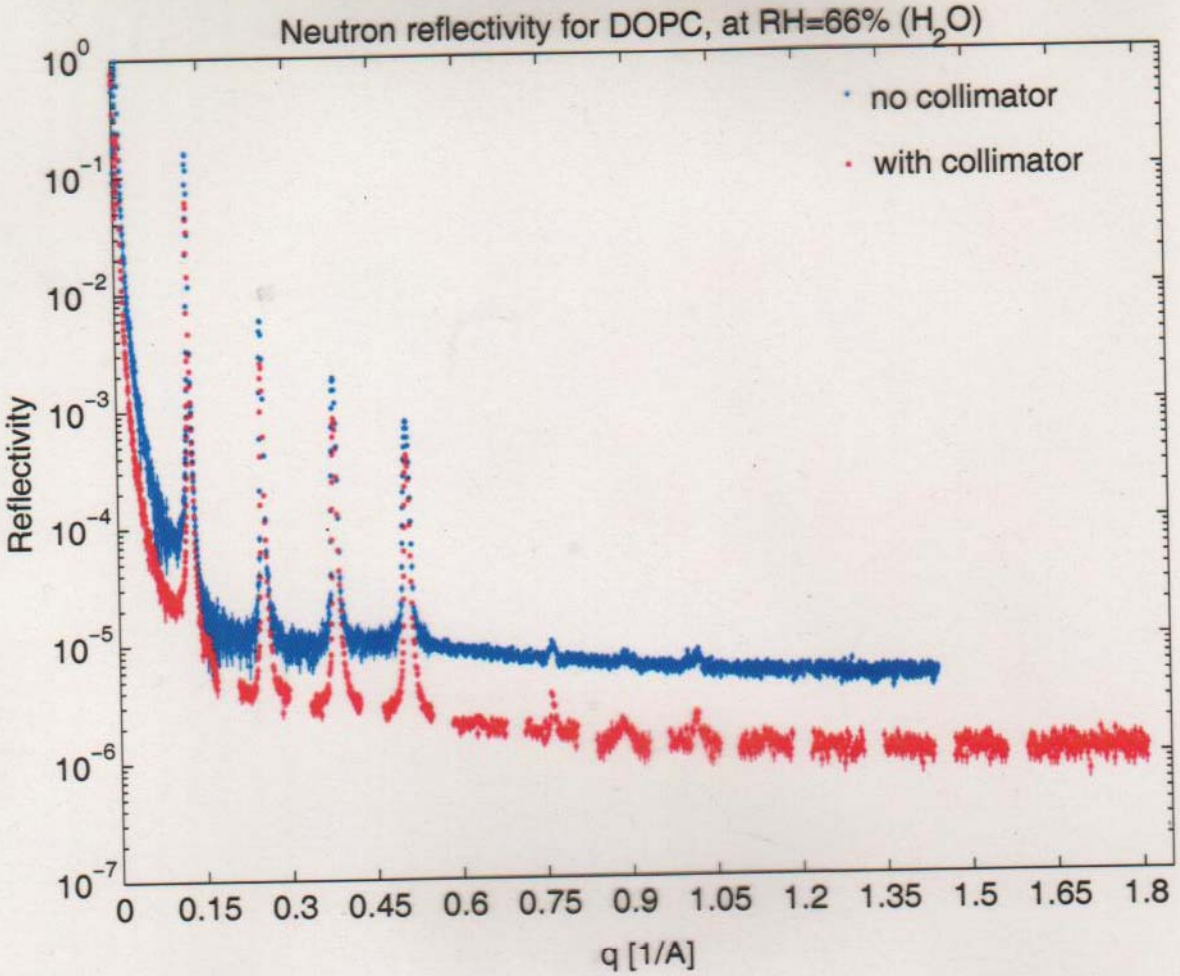
Neutron reflectivity for DOPC, at RH=66% (H_2O)
no collimator
with collimator
Reflectivity
10^{0}
10^{-1}
10^{-2}
10^{-3}
10^{-4}
10^{-5}
10^{-6}
10^{-7}
0 0.15 0.3 0.45 0.6 0.75 0.9 1.05 1.2 1.35 1.5 1.65 1.8
q [1/A]

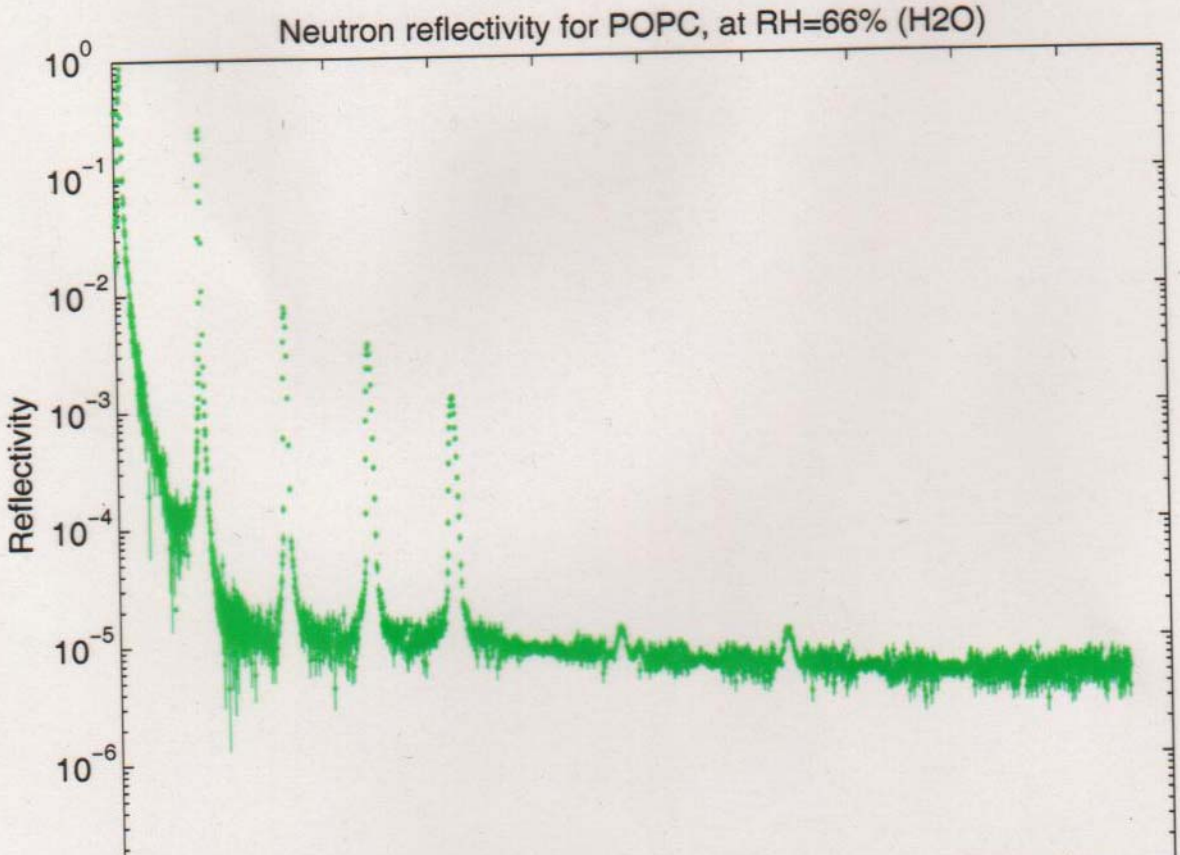
Neutron reflectivity for POPC, at RH=66% (H2O)
Reflectivity
10^{0}
10^{-1}
10^{-2}
10^{-3}
10^{-4}
10^{-5}
10^{-6}

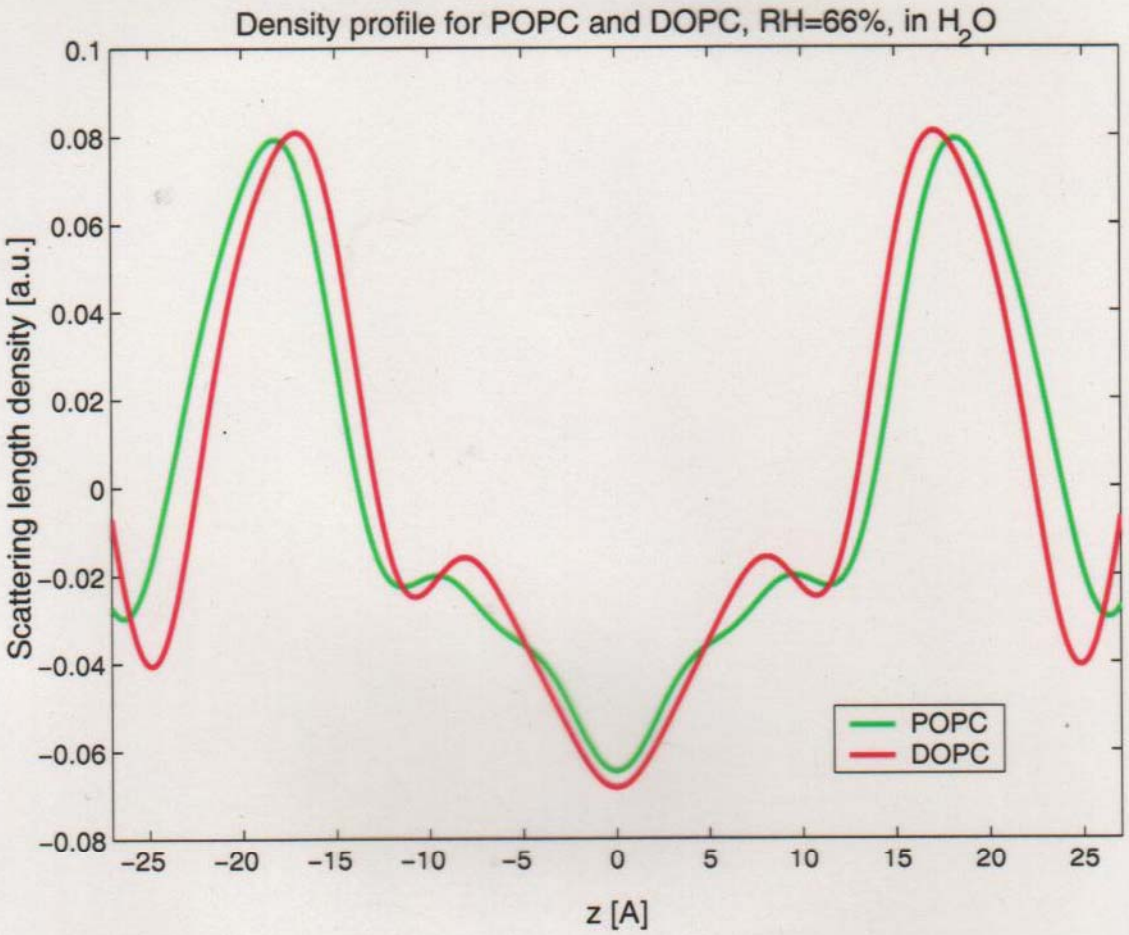

DOPC

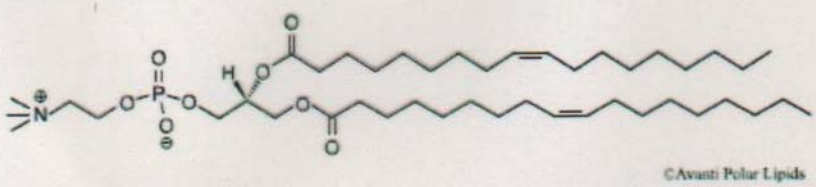

POPC

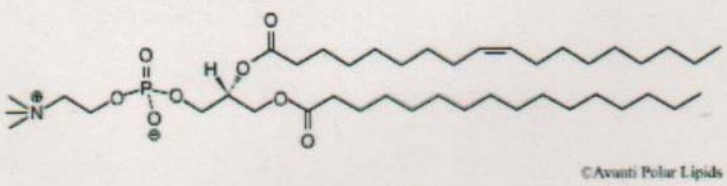

Ella Mihailescu, Francisco Castro-Roman,
Ryan Benz, Stephen White, UC Irvine

Phase Sensitive Neutron Reflectometry on a Water-Cushioned Biomembrane-Mimic

Biomimetic membranes have been developed as models of living cell membranes, and this has applications in the quest for biocompatibility of inorganic materials in biologically active mediums, such as coatings for artificial organs. A membrane consists of a lipid bilayer (two lipid layers) where hydrophobic carbon chains form the inside of the membrane and their polar head groups the interface with the aqueous surrounding medium. A supported membrane-mimic consists of a lipid-like bilayer, typically attached to a single-crystal substrate, with access to water only at the top surface [1, 2]. Here we use neutron reflectometry to study a system in which water has access to both sides of a membrane-mimic attached to such a substrate, thus making the system a closer mimic to a real cell membrane.

The system devised by Liu *et al.* [3] consists of a water-swellable polyelectrolyte that electrostatically binds to the substrate and acts as a "cushion" for the membrane, not unlike the cytoskeletal support found in actual mammalian cell membranes. The lower half of the membrane-mimic is a terpolymer that attaches to the polyelectrolyte. A phospholipid layer forms on top of the terpolymer and the bilayer is finally chemically crosslinked for added stability. The system is shown schematically in Fig. 1.

Neutron reflectivity measurements were performed at the NG-1 vertical stage reflectometer to obtain the compositional profile at every step of the assembling process of the membrane-mimic which consisted of three stages: a) polyelectrolyte multilayer (PE), b) polyelectrolyte multilayer plus terpolymer (PE+TER), and c) polyelectrolyte multilayer plus terpolymer plus phospholipid layer (PE+TER+PC) [4]. The spatial resolution attained was approximately 10 Å, about half the thickness of a membrane bilayer, making it possible to distinguish the two layers of a membrane but not the structure of a single layer.

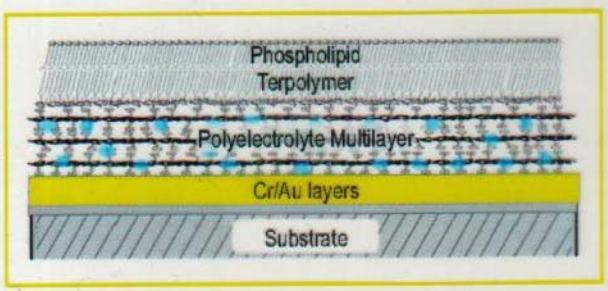

Fig. 1. Schematic diagram of a biomimetic membrane. The phospholipid layer at the top combines with the terpolymer layer to form a membrane-mimic that in turn resides on the water (blue dots) permeable "cushion" polyelectrolyte multilayer. The latter attaches electrostatically to the Au-capped substrate.

A unique compositional profile of the biomimetic film with no a priori knowledge of the sample's composition is obtained by measuring the reflectivity of equivalent samples made onto two substrates [5]. The substrates used were single crystal silicon (Si) and sapphire (Al_2O_3) coated with chromium (Cr) and then a gold (Au) layer to allow the polyelectrolytes to bind to a similar surface on both wafers.

Figure 2 shows the compositional profiles for the PE, PE+TER and PE+TER+PC assemblies in a D_2O atmosphere at 92 % relative humidity. The figure shows that the hydration of the PE layer is almost unaffected by the addition of the terpolymer and the phospholipid layer. Also, upon the addition of the phospholipid layer to the PE+TER assembly, the composite PE+TER+PC assembly shows an increase in thickness of approximately 30 Å, consistent with the formation of a single phospholipid layer at the surface. It is also clear that the addition of a phospholipid layer onto the terpolymer layer rearranges this region

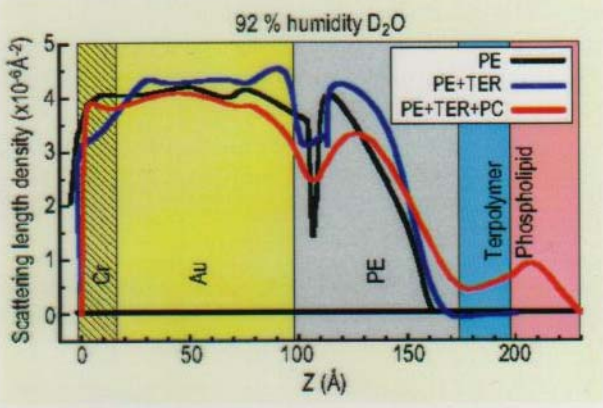

Fig. 2. Compositional profile of biomimetic membrane in a D_2O atmosphere at 92 % relative humidity at various stages of assembly on Au-capped substrate: only polyelectrolyte (PE), polyelectrolyte and terpolymer (PE+TER), polyelectrolyte, terpolymer and phospholipid (PE+TER+PC). The compositional profile is given by the scattering length density, SLD, profile when using neutrons.

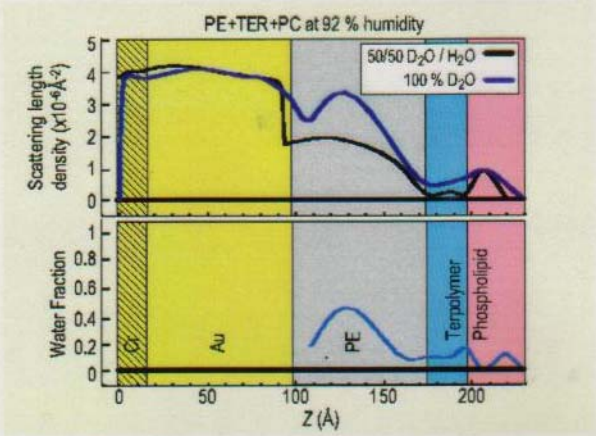

Fig. 3. Scattering length density profiles (top) and water fraction (bottom) for PE+TER+PC under indicated conditions.

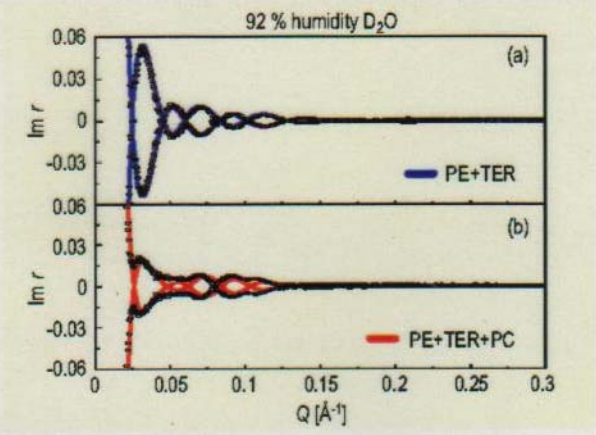

Fig. 4. Imaginary part of the complex reflectivity, Im $r(Q)$, data (symbols) and calculated curves (lines) obtained from the SLD profiles for the PE+TER and the PE+TER+PC assemblies shown in Fig. 2.

significantly, since the terpolymer layer only becomes apparent after the phospholipid layer is added. It is possible to verify with an independent technique (contact angle) that the terpolymer was in fact deposited because it forms a hydrophobic outer layer. The outer surface becomes hydrophilic once the phospholipid layer is deposited onto the terpolymer layer.

Figure 3 (top) shows the profile for the PE+TER+PC assembly under 92 % relative humidity in 100 % D_2O and in 50/50 D_2O/H_2O. The overall thickness change due to the intake of water, in going from dry (not shown) to 92 % relative humidity, was found to be 20 Å. Figure 3 (bottom) shows the water fraction in the assembly under 92 % relative humidity. This is obtained by assuming that the distribution of each component in the layers is unaffected by having either D_2O or 50/50 D_2O/H_2O. From the figure it can be seen that the polyelectrolyte multilayer has a 40 % water uptake. This is a significant amount of water, which suggests that the polyelectrolyte multilayer can work as a "cushion" for membrane-mimetic systems. The terpolymer and the phospholipid layers contain an average of 10 % water, which is also significant, suggesting that these layers are not tightly packed.

The method of making equivalent samples on two substrates to obtain a unique compositional profile has a built-in congruency test, particularly useful in checking the reproducibility of the samples as well as the quality of the films. The test is to compare the calculated imaginary part of the complex reflectivity from the obtained profile with the corresponding data, as is shown in Fig. 4 for the PE+TER and PE+TER+PC assemblies. From Fig. 4 it is concluded that the PE+TER samples are homogenous and essentially identical while for the PE+TER+PC assembly, the absence of true zeros, as indicated by the calculated curve, is suggestive of a small degree of sample inhomogeneity.

The system from Liu *et al.* has many characteristics desirable in a biomimetic membrane. It is a single membrane-mimic attached to a significantly hydrated soft "cushion" support that allows some membrane proteins to function. Thrombomodulin, a membrane protein relevant to blood-clotting, is being studied in this membrane-mimic environment to further develop biocompatible coatings for artificial organs [6].

References

[1] E. Sackmann, Science **271**, 43 (1996).

[2] A. L. Plant, Langmuir **15**, 5128 (1999).

[3] H. Liu, K. M. Faucher, X. L. Sun, J. Feng, T. L. Johnson, J. M. Orban, R. P. Apkarian, R. A. Dluhy, E. L. Chaikof, Langmuir **18**, 1332 (2002).

[4] U. A. Perez-Salas, K. M. Faucher, C. F. Majkrzak, N. F. Berk, S. Krueger, E. L. Chaikof, Langmuir **19**, 7688 (2003).

[5] C. F. Majkrzak, N. F. Berk, U. A. Perez-Salas Langmuir **19**, 1506 (2003).

[6] J. Feng, P. Y. Tseng, K. M. Faucher, J. M. Orban, X. L. Sun, E. L. Chaikof, Langmuir **18**, 9907 (2002).

U. A. Perez-Salas
NIST Center for Neutron Research
National Institute of Standards and Technology, Gaithersburg, MD 20899-8562

K. M. Faucher
Emory University School of Medicine, Atlanta, GA 30322

C. F. Majkrzak, N. F. Berk, S. Krueger
NIST Center for Neutron Research
National Institute of Standards and Technology
Gaithersburg, MD 20899-8562

E. L. Chaikof
Emory University School of Medicine
Atlanta, GA 30322

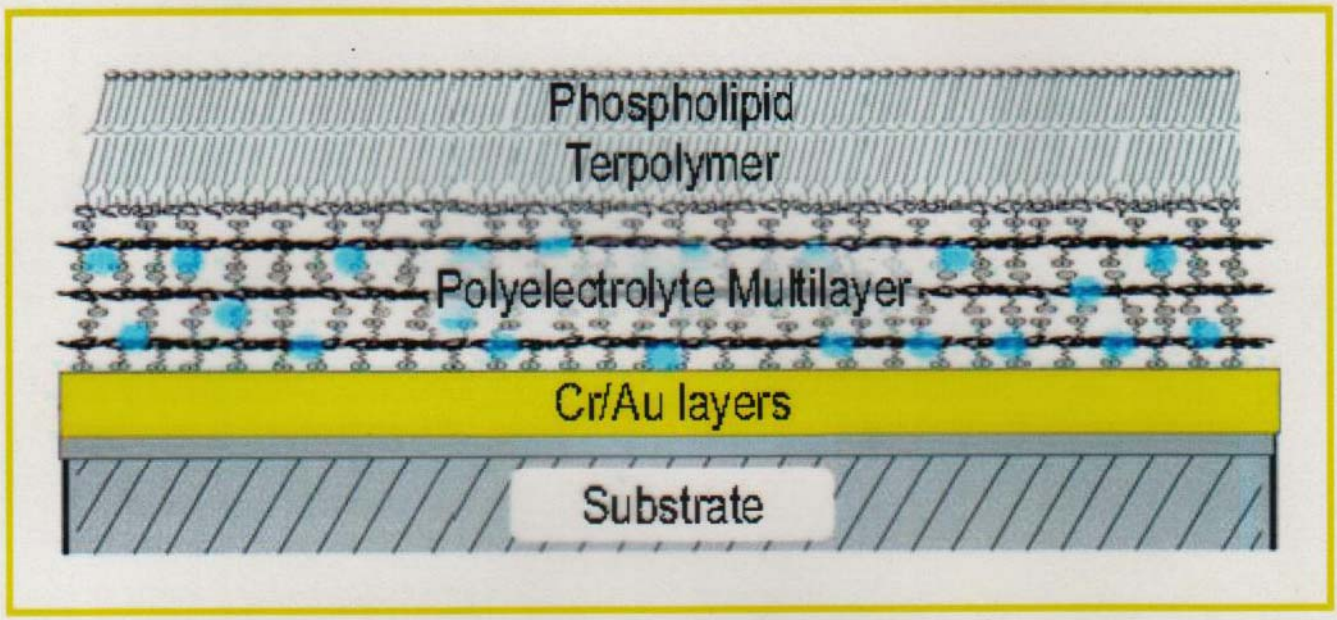

Fig. 1. Schematic diagram of a biomimetic membrane. The phospholipid layer at the top combines with the terpolymer layer to form a membrane-mimic that in turn resides on the water (blue dots) permeable "cushion" polyelectrolyte multilayer. The latter attaches electrostatically to the Au-capped substrate.

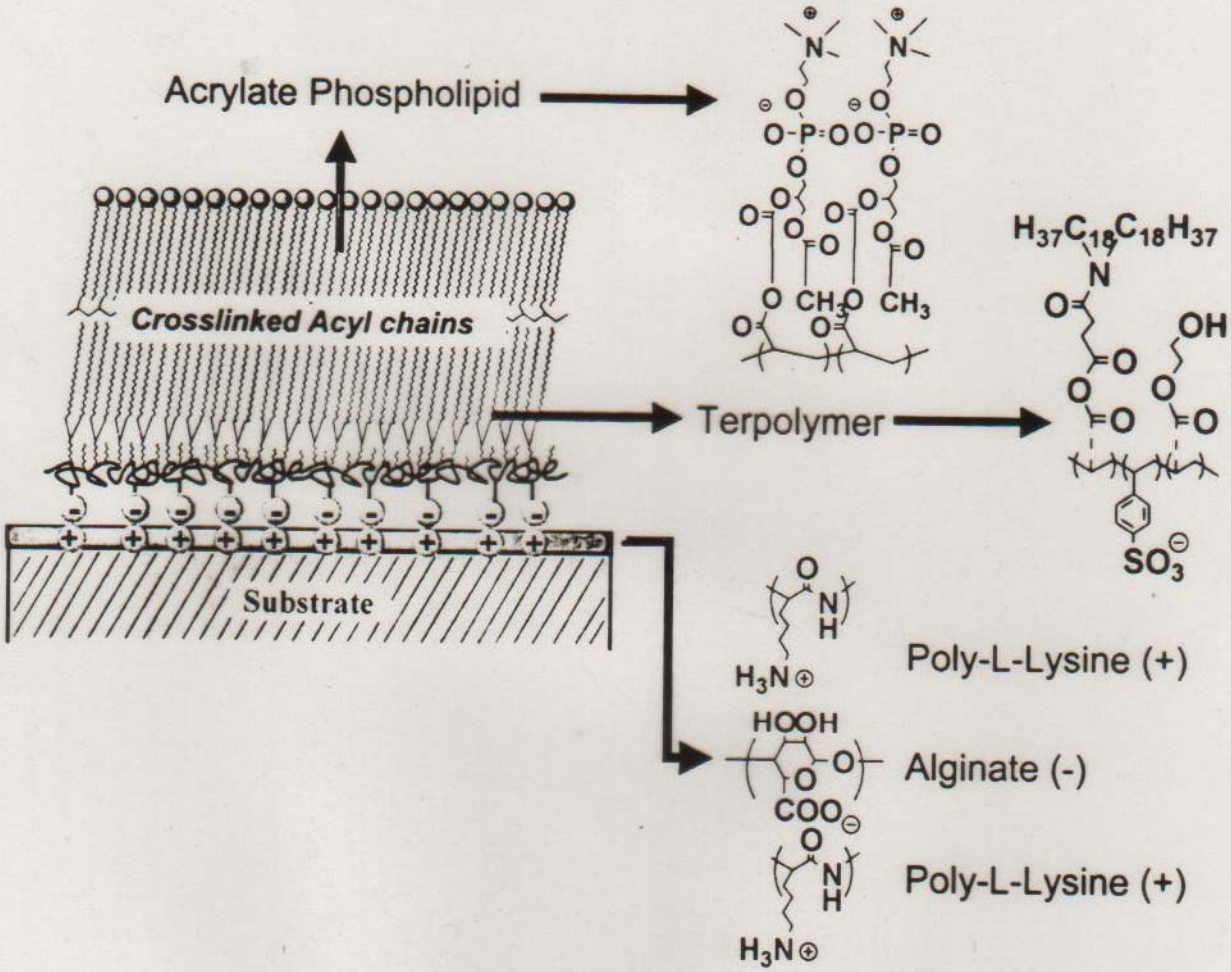

Figure 1:

1 Schematic representation the terpolymer (TER)-acrylate phospholipid (PC) membrane mimic supported on a polyelectrolyte multilayer(PE) "cushion". . . . . .

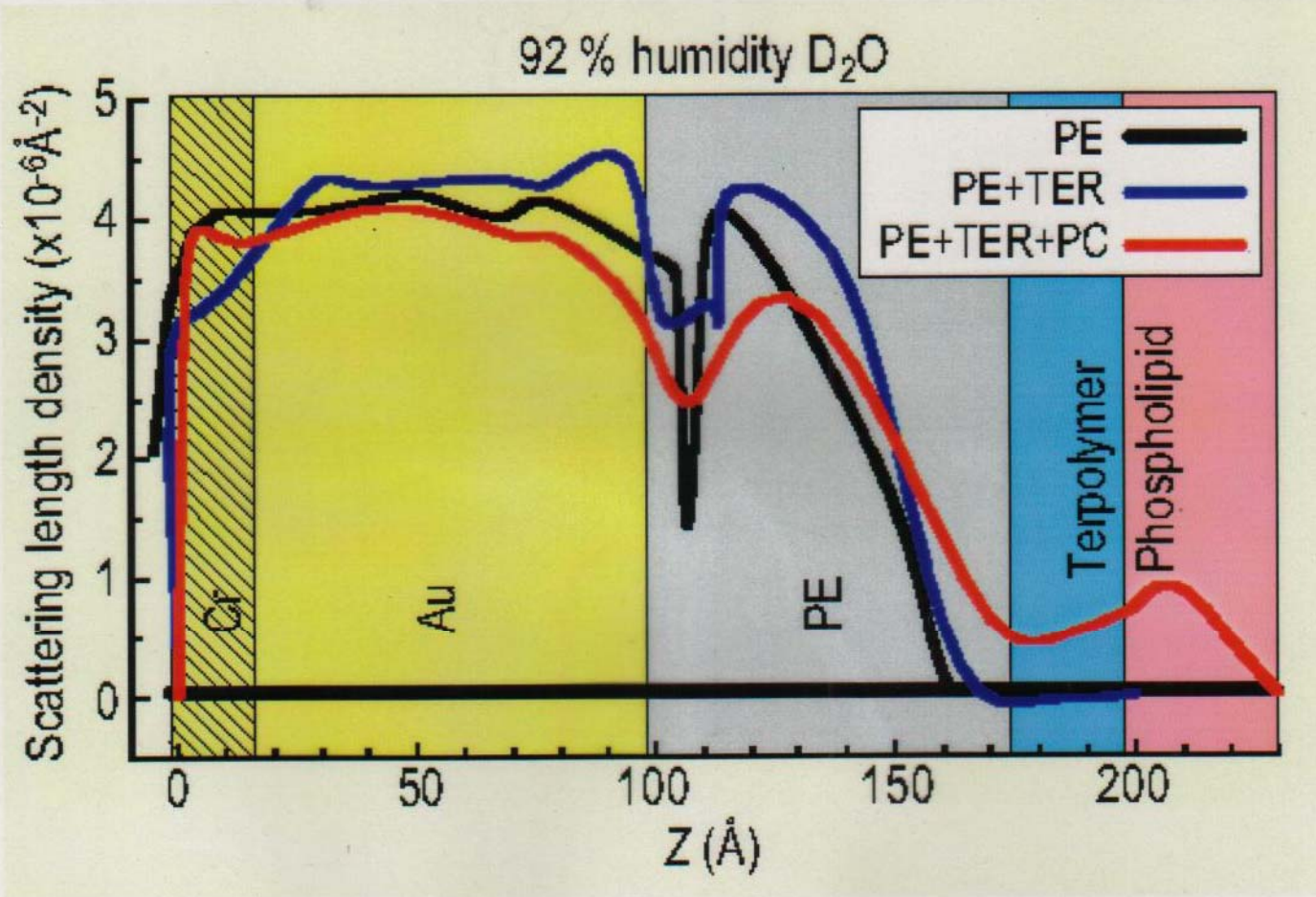

Fig. 2. Compositional profile of biomimetic membrane in a D_2O atmosphere at 92 % relative humidity at various stages of assembly on Au-capped substrate: only polyelectrolyte (PE), polyelectrolyte and terpolymer (PE+TER), polyelectrolyte, terpolymer and phospholipid (PE+TER+PC). The compositional profile is given by the scattering length density, SLD, profile when using neutrons.

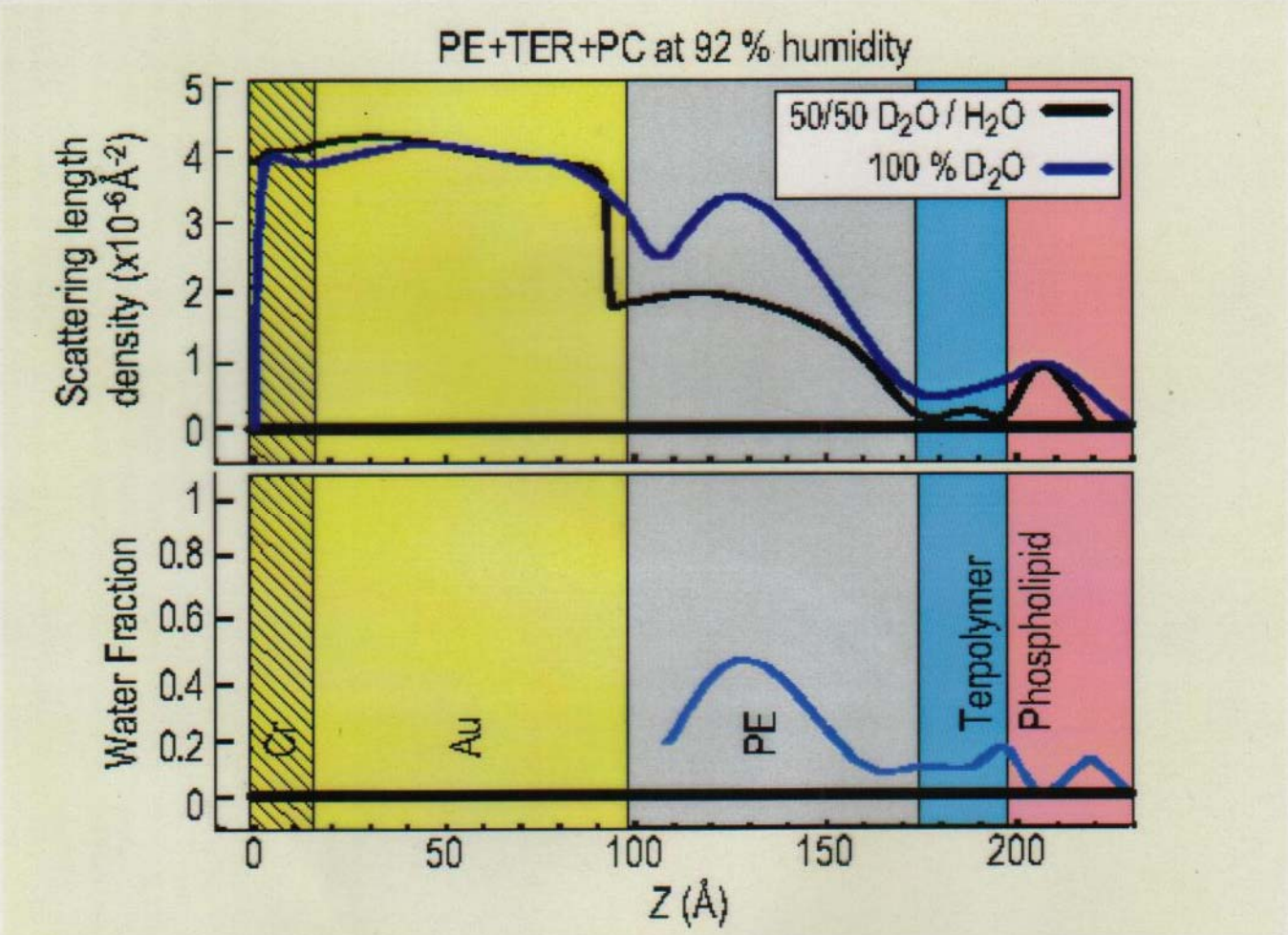

Fig. 3. Scattering length density profiles (top) and water fraction (bottom) for PE+TER+PC under indicated conditions.

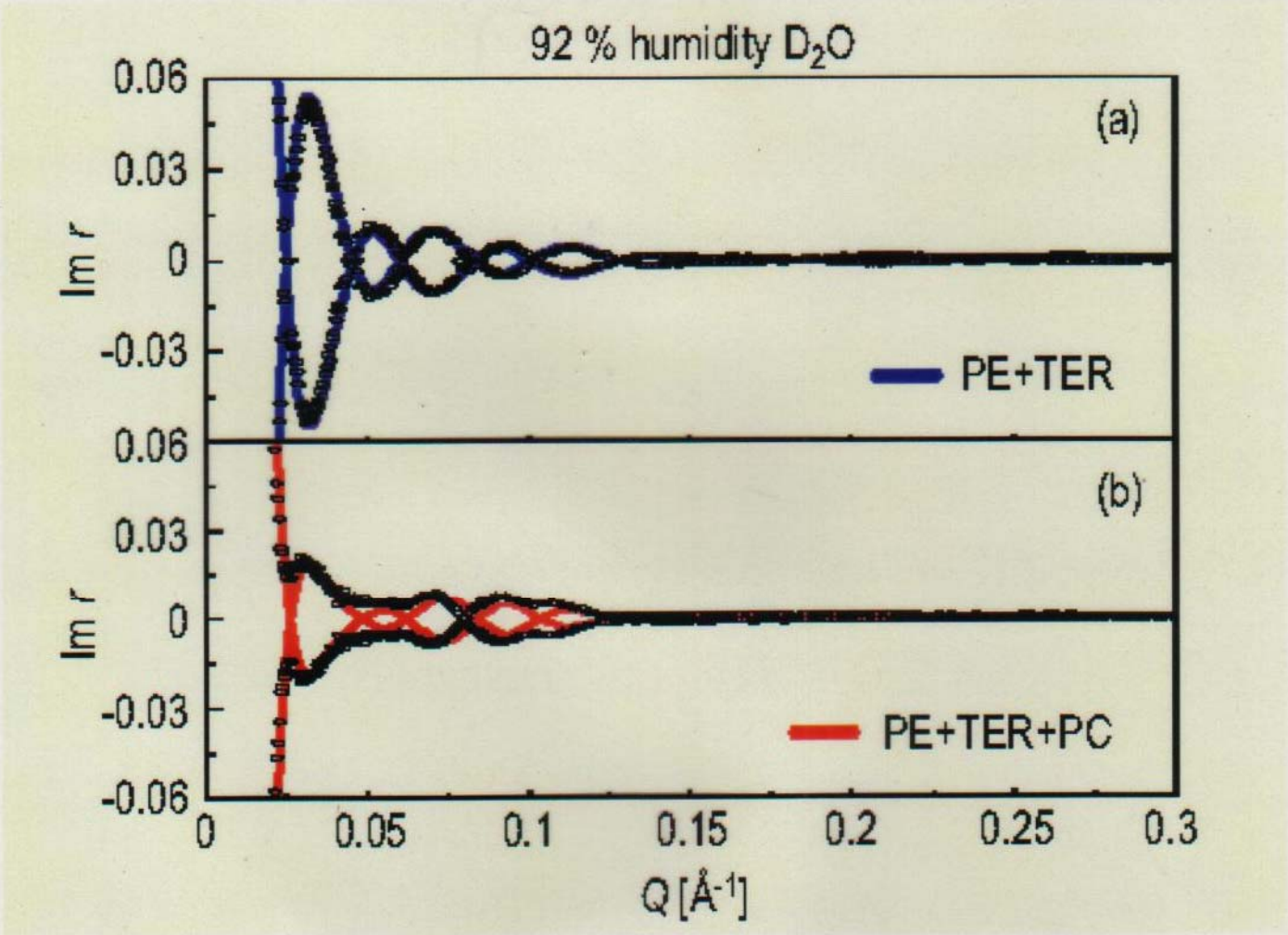

Fig. 4. Imaginary part of the complex reflectivity, Im $r(Q)$, data (symbols) and calculated curves (lines) obtained from the SLD profiles for the PE+TER and the PE+TER+PC assemblies shown in Fig. 2.